

Analysis of reach-scale sediment process domains in glacially-conditioned catchments using self-organizing maps

Kristen L. Underwood^{a,*}, Donna M. Rizzo^a, Mandar M. Dewoolkar^a, Michael Kline^{b,1}

^a Department of Civil and Environmental Engineering, Votey Building, 33 Colchester Ave., University of Vermont, Burlington, VT 05405, USA

^b Vermont Agency of Natural Resources, Department of Environmental Conservation, One National Life Drive, Montpelier, VT, 05620-3520, USA

ARTICLE INFO

Article history:

Received 31 December 2019

Received in revised form 28 February 2021

Accepted 2 March 2021

Available online 5 March 2021

Keywords:

Process domain
channel classification
Sediment transport
Self-Organizing Map

ABSTRACT

Given the limited resources available for managing erosion hazards and addressing water quality impairment along rivers, stakeholders engaged in water resource management would benefit from tools to identify those river reaches most prone to adjustment and which disproportionately load sediment to receiving waters. The extent and rate of vertical and lateral channel adjustments in response to natural and human disturbances vary considerably across space and time; and this complexity and nonlinearity introduce challenges for classification or modeling of river reaches using conventional statistical techniques. The Self-Organizing Map (SOM) is a data-driven computational tool with advantages for clustering or classifying multivariate observations and for exploratory data analysis and visualization of complex, nonlinear systems. We applied a SOM to cluster multivariate stream geomorphic assessment data into reach-scale sediment process domains for 193 river reaches in glacially-conditioned catchments of northeastern US using field- and GIS-derived hydraulic and geomorphic parameters. The reaches comprised a range of channel types from confined to unconfined, steep- to shallow-gradient, mid-to-high order, and bedrock to alluvial channels. Fifteen variables were identified that meaningfully separated reaches into seven sediment regimes, following a two-stage application of the SOM. A coarse-tune SOM identified sediment regime classes at the supply-limited and transport-limited extremes of a continuum, including bedrock channels and confined, steep-gradient reaches as well as braided, depositional channels at alluvial fan or delta settings. A second-stage, fine-tune SOM nuanced differences in sediment production and transport for unconfined reaches with varying degrees of floodplain disconnection resulting from natural or human stressors. This classification framework is transferable to other hydroclimatic regions, with consideration of additional or alternate independent variables unique to those regions, and can provide valuable insights for river management to promote flood resiliency, restore water quality and improve instream and riparian habitats.

© 2021 Elsevier B.V. All rights reserved.

1. Introduction

River reaches undergoing excessive rates of adjustment pose hazards to infrastructure and public safety, and contribute to degraded water quality and compromised instream and riparian habitats. In glacially-conditioned mountainous areas, rivers have differing vulnerabilities to adjustment given their topographic setting, variable coupling of hillslope and channel processes, and reworking of glaciogenic sediments (Church and Ryder, 1972; Ballantyne, 2002). The geologic and glacial history have imparted longitudinal and lateral variations in valley setting and network position, as well as discontinuities in channel form and process (Rice and Church, 1998; Toone et al., 2014; Phillips

and Desloges, 2014a) that influence the dynamics of sediment erosion, transport and deposition (Nanson and Croke, 1992; Fryirs et al., 2007). Human disturbances over the last 250 years have also altered patterns of water and sediment routing through the landscape (Leopold, 1994; Noe and Hupp, 2005; Walter and Merritts, 2008). As a consequence, rivers have become laterally and vertically disconnected from their floodplains, leading to reduced floodplain storage and increased streambank and channel erosion (Brierley and Fryirs, 2005; Kline and Cahoon, 2010).

Water resource managers need tools to identify river reaches most prone to adjustment and which disproportionately load sediment to receiving waters. However, significant challenges exist for classification and prediction, given the complexity of sediment dynamics. Patterns of sediment flux and channel adjustment exhibit high variability across spatial and temporal scales (Walling, 1983; Fryirs, 2013), as a function of both watershed-level and reach-level processes that alter flow and sediment inputs, as well as stream power and boundary resistance. Many factors, including the geologic setting, climate, hydrology,

* Corresponding author.

E-mail addresses: Kristen.Underwood@uvm.edu (K.L. Underwood),

Donna.Rizzo@uvm.edu (D.M. Rizzo), Mandar.Dewoolkar@uvm.edu (M.M. Dewoolkar).

¹ Present Address: Fluvial Matters, LLC, 401 S. Bear Swamp Rd., Middlesex, VT 05602, USA.

vegetation, and land use, combine in nonlinear ways to adjust reach-scale channel dimensions, profile and planform over time (Benda and Dunne, 1997; Fryirs, 2013). The present channel form is the manifestation of various channel-floodplain processes occurring in response to a suite of natural and human disturbances over a range of flows (Pickup and Rieger, 1979; Wohl, 2018). Rivers are integrating these myriad of stressors overlapping in time and space, and may adjust to an external stressor(s) in complex ways based on: the magnitude, intensity and duration of the stressor; lag effects; intrinsic and extrinsic thresholds; self-reinforcing or self-limiting feedbacks; and the presence of antecedent conditions or contingencies (Bull, 1979; Chappell, 1983; Phillips, 2003; Toone et al., 2014). Despite these complexities and the uncertain causal factors, the present channel-floodplain form warrants classification to communicate the associated consequences for flood erosion hazard, water quality and ecological integrity. Classification is also useful for highlighting reach sensitivity to future disturbances or to hydrologic regime change that may be associated with projected increases in magnitude, frequency, and duration of extreme events (Collins, 2009; Guilbert et al., 2014, 2015).

Various field assessment techniques help to classify river reaches in terms of their stability or sensitivity to adjustment, following the assumption that dominant adjustment process and degree of stability may be inferred from observed channel form (Pfankuch, 1975; Nanson and Croke, 1992; Rosgen, 1996; Montgomery and Buffington, 1997; Raven et al., 1998; Brierley and Fryirs, 2005; Rinaldi et al., 2013). Insights gained from these assessments have led to the theory that river networks comprise a longitudinal array of hydrogeomorphic units of relatively uniform composition, structure, and function, or “process domains” that differentially impact sediment connectivity (Montgomery, 1999; Brardinoni and Hassan, 2007; Weekes et al., 2012; Lisenby and Fryirs, 2016).

Parametric statistical methods have been employed to examine correlations between dominant adjustment process and various geomorphic metrics, such as total or specific stream power (Bizzi and Lerner, 2013; Parker et al., 2014; Gartner et al., 2015; Lea and Legleiter, 2016; Yochum et al., 2017); valley confinement (Thompson and Croke, 2013; Surian et al., 2016; Righini et al., 2017; Weber and Pasternack, 2017); and channel geometry (Buraas et al., 2014). Geographic Information Systems (GIS) and high-resolution digital elevation models have enabled remotely-sensed metrics to augment field-based assessment. Large, multi-parameter data sets help to examine interactions among a suite of factors governing channel-floodplain form and process. Multivariate statistical techniques (e.g., principal components analysis, k-means, discriminant analysis, logistic regression, and regression trees) help with data reduction and unraveling the association of channel and floodplain form with process (Flores et al., 2006; Brardinoni and Hassan, 2007; Phillips and Desloges, 2014b; Livers and Wohl, 2015). However, these methods are predicated on linear relationships between variables, which often do not describe geomorphic data well. Moreover, their application assumes the data are normally distributed, while geomorphic variables often do not reliably conform to a Gaussian distribution.

Because sediment erosion, transport and deposition processes are a manifestation of multiple factors and nonlinear interactions, Phillips (2003) advocated for the application of nonparametric, computational tools to model nonlinear, complex dynamics. Artificial neural networks are well-suited for nonlinear processes, and handle nonparametric data of varying types (e.g., continuous, ordinal, nominal) and scales. The Self-Organizing Map (SOM) is one such neural network for clustering or classification of multivariate observations (Kohonen, 2013). SOMs have demonstrated superior performance over parametric methods where data contain outliers or exhibit high variance (Mangiameli et al., 1996), and have particular advantages over other methods for data visualization and interpretation (Alvarez-Guerra et al., 2008). SOMs have been used to classify or cluster multivariate environmental data, including instream species richness (Park et al., 2003), fish

community distribution patterns (Stojkovic et al., 2013), lake chemistry data associated with harmful algal blooms (Pearce et al., 2011, 2013), and riverine habitats (Fytillis and Rizzo, 2013). Previous research (Besaw et al., 2009) applied a SOM to reach-based geomorphic assessment data to classify reach-level sensitivity, or the likelihood for channel adjustment (vertical or lateral adjustment) in response to natural or human disturbance(s). However, the authors are not aware of the SOM being applied to classify sediment regime of river reaches.

In this work, we use SOMs to characterize and predict the spatial variation in fluvial sediment regimes. Consistent with Wohl et al. (2015), we define a sediment regime as a pattern of “inputs and outputs of mobile sediment from a length of channel and storage of sediment within the channel and floodplain over a specified time interval”. The research objectives are to: (1) apply the SOM to cluster commonly-assessed stream geomorphic parameters and define a continuum of sediment regimes, using catchments from the glacially-conditioned northeastern United States as a test case; (2) assess this data-driven clustering tool’s ability to emulate the decision-making of stream geomorphic experts following an existing reach-scale classification of sediment regimes (Kline, 2010) with a goal to refine the classification and enable future automation; and (3) illustrate the utility of the SOM for data visualization and interpretation.

2. Study area

Our study comprises 193 river reaches located in six relatively undeveloped ($\leq 5.3\%$) catchments dispersed across the state of Vermont in the northeastern United States (Fig. 1; Supplementary Table S1), and chosen to represent a mix of biogeophysical regions (Stewart and MacClintock, 1969). Study reaches range from 95 to 4724 m in length with upstream drainage areas between 0.93 and 302 km² (Table S2). This previously-glaciated landscape consists of a mix of deposits ranging from glacial tills, glaciofluvial, and glaciolacustrine sediments and alluvial fans, deltas, and post-glacial stream terraces (Stewart and MacClintock, 1969). The bedrock underlying these soil parent materials generally consists of erosion-resistant crystalline and metamorphosed rocks of the highlands (e.g., gneiss, phyllites, schist, schistose greywacke, slate, granite) and less-erosion-resistant limestones and dolostones in the valleys (Ratcliffe et al., 2011). Generally, bedrock channels in the headwaters grade to mixed bedrock-alluvial and alluvial channels in the lowlands. Where the river impinges upon hillslopes of glacial till or high terraces of glacial origin (e.g., kame, delta, or lacustrine deposits), landsliding can contribute sediment and large woody debris to the channel (Dethier et al., 2016).

Historically, European settlement and the associated deforestation (Foster and Aber, 2004) generated high sediment yields from denuded hillslopes, leading to renewed aggradation in many alluvial reaches (Brakenridge et al., 1988; Bierman et al., 1997). Subsequent reforestation has reduced sediment yields, contributing to channel incision and widening (Bierman, 2010; Schumm and Rea, 1995). Channelization, berming, armoring, and diversion of rivers during development, have locally disconnected river channels from the adjacent floodplains (Poff et al., 1997; Kline and Cahoon, 2010). Dams were historically operated at bedrock knick-points in the headwaters to power local mills (Thompson and Sorenson, 2000); however, these small impoundments were typically breached during flood events of the 19th and 20th century. At present, four dams remain on the studied reaches, but have limited impoundments and operate in run-of-river mode. Thus, longitudinal hydrologic connectivity is maintained, but these grade controls may represent a sediment transport discontinuity to varying degrees.

A humid temperate climate characterizes the region, with mean annual precipitation ranging from over 1270 mm along the north-south trending spine of the Green Mountains to a low of 813 mm in the Champlain Valley (Randall, 1996). Spring and fall rains are common, and saturation-excess overland flow conditions dominate during these

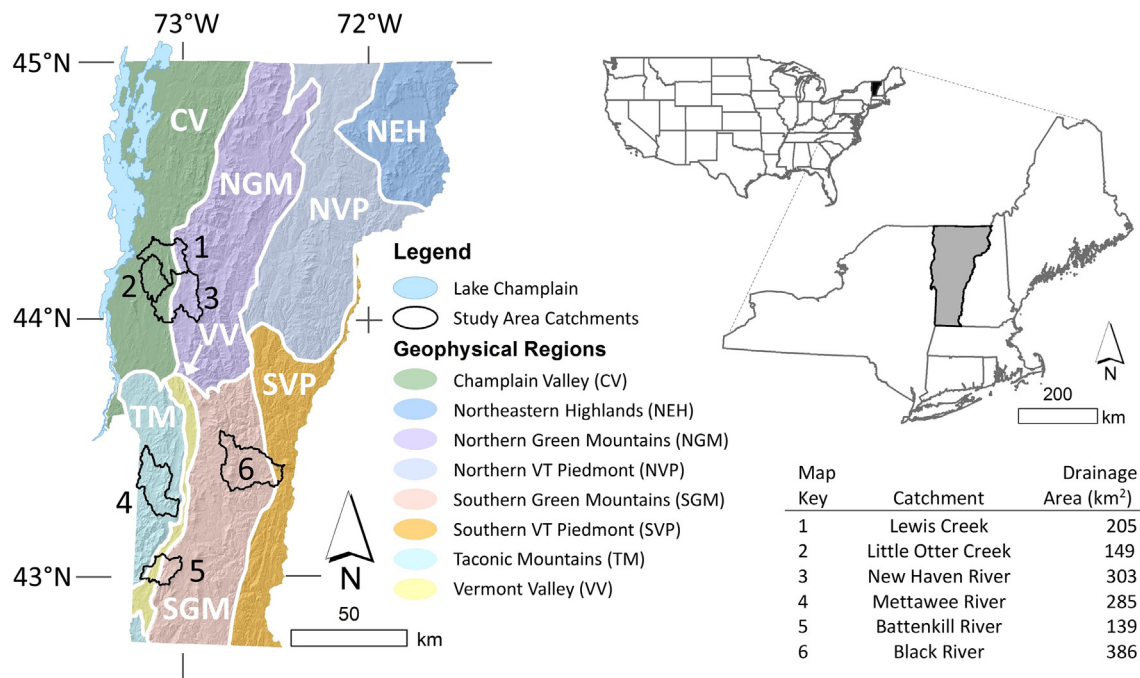


Fig. 1. Location of study area watersheds across biogeophysical regions in Vermont.

months, leading to variable hydrologic source areas (Dunne and Black, 1970). A majority of the total annual flow in the studied rivers occurs from snow- and ice-melt to late spring in a typical year, due to the occurrence of spring rains falling on saturated or frozen ground, melting of the snow pack stored in higher elevations, and low evapotranspiration rates prior to leafing of deciduous vegetation (Shanley and Denner, 1999). The peak annual flow (1 to 1.5-year recurrence interval) most often occurs during the spring months, although occasionally in the fall or summer (USGS, 2018).

3. Methods

Research progressed in multiple phases: (1) assessments to gather geomorphic and hydraulic variables; (2) assignment of sediment regime classification; (3) exploratory data analysis; and (4) the application and (5) training of a SOM clustering algorithm to replicate and refine sediment regime classifications assigned by experts.

3.1. Assessment of geomorphic condition

Reach-scale geomorphic and hydraulic data were compiled from existing remote-sensing resources and field-based assessment for 193 river reaches in six catchments (Fig. 1). Assessed reaches were located along confined to unconfined, steep- to shallow-gradient, mid-to-high order channels that ranged from bedrock to alluvial in nature (Table S2, Fig. S1). Reaches affected by impoundments (artificial or beaver-constructed) or wetland conditions were not included in assessments. River reaches were assessed during a relatively quiescent period (2004 through 2011) between significant flood events. The six study area catchments were affected by an extreme event, a state-wide flood of significance (recurrence interval ranging from 25 to 500+ years) in August 2011 during Tropical Storm Irene (USGS, 2018). Except for three of the 193 reaches (1.6%), geomorphic data from our study catchments were collected before this extreme event, and these three reaches were located in catchment #3 (Fig. 1) where Tropical Storm Irene generated only a 50-yr flood (VT Agency of Natural Resources, 2017).

Stream geomorphic assessments were conducted following protocols (Kline et al., 2009) developed by the Vermont Agency of Natural Resources relying on several resources (Wolman, 1954; Pfankuch, 1975; Nanson and Croke, 1992; Harrelson et al., 1994; Rosgen, 1996; Montgomery and Buffington, 1997; Knighton, 1998). These quality-assured and peer-reviewed protocols (Besaw et al., 2009; Somerville and Pruitt, 2004) have been developed and applied to classify river reaches in terms of their dominant adjustment process, stage of channel evolution, and sensitivity to future adjustment (Kline et al., 2009). Reaches were defined as channel lengths of consistent confinement ratio (confined, semiconfined or unconfined) within which other channel parameters (slope, sinuosity, and bedform) were generally similar – a reach definition conforming to that employed by others (Frissell et al., 1986; Brierley and Fryirs, 2005; Rinaldi et al., 2013; Surian et al., 2016). Additionally, minimum reach lengths were generally greater than 20 times the bankfull width (Montgomery and Buffington, 1997). Following initial identification through desk-top assessment of topographic and photographic resources, reach delineations were confirmed through direct observation, where sub-reaches of alternate slope or valley confinement may not have been apparent at the typical scale (1:24000) of remote-sensing resources used in this study. In some cases, field assessment also defined sub-reaches marked by discontinuities (e.g., bedrock grade controls or impoundments) or distinct differences in dominant substrate material or adjustment process (Kline et al., 2009). For clarity of presentation, these sub-reaches are referred to as reaches in this work. Various geomorphic and hydraulic metrics were compiled for each reach (including List A in Table 1) using a combination of remote-sensing and field-based assessment (see Supplementary materials). Based on this information, each reach was classified by stream type (Montgomery and Buffington, 1997; Rosgen, 1996), dominant style of vertical (degradation or aggradation) and/or planform (widening, narrowing or lateral migration) adjustment, and channel evolution model and stage (Schumm et al., 1984).

Additional variables were derived for this study to evaluate their effectiveness to describe sediment regimes and to cluster reaches of similar character. Various methods for estimating stream power (Parker et al., 2011, 2014) and tractive force (Andrews, 1983; Ferguson, 2005)

Table 1
Geomorphologic and hydraulic variables used to classify sediment regime.

A	B	C	Variable	Description	Units	Transformation
✓	✓	✓	Slope, S	Channel slope	[%]	Log S ^a
✓	✓	✓	Valley Confinement, VC	Valley width/bankfull width	[–]	Log VC ^a
✓	✓	✓	Incision Ratio, IR	Low-bank height/bankfull channel height	[–]	Log IR ^b
✓	✓	✓	Entrenchment Ratio, ER	Floodprone width/bankfull width	[–]	Log ER ^b
✓	✓	✓	Width _{bkfl} to Depth _{mn} ratio, W/D	Bankfull width/mean bankfull depth	[–]	Log W/D ^b
✓	✓	✓	Median grain size diameter, D50	Median grain size diameter from riffle or step pebble count, i.e., 50th percentile of the grain size distribution	[mm]	$\sqrt{D50}$ ^b
✓	✓	✓	Percent Armoring, pArm	Length armoring normalized to reach length	[%]	Arcsin(sqrt(pArm)) ^b
✓	✓	✓	# Depositional Bars, nBars	Number of deposition bars normalized to reach length	[#/km]	\sqrt{nBars} ^b
✓	✓	✓	# Flood Chutes, nFCs	Number of flood chutes normalized to reach length	[#/km]	\sqrt{nFCs} ^b
✓	✓	✓	Valley Confinement Ratio, VCrat	VC of subject reach/VC of upstream reach	[–]	Log VCrat ^a
✓	✓	✓	Grain Size Distribution, D84-D16	Range of two standard deviations around the median, computed as the 84th percentile minus the 16th percentile of the grain size distribution	[mm]	Log D84-D16 ^b
✓	✓	✓	Specific Stream Power, SSP	Unit bed area stream power	[W m ⁻²]	Log SSP ^b
✓	✓	✓	SSP Balance, SSPbal	SSP of subject reach/SSP of upstream reach	[–]	Log SSP bal ^b
✓	✓	✓	Width ratio, Wrat	Regime bankfull width/measured bankfull width	[–]	Wrat ^b
✓	✓	✓	Mean Depth ratio, Drat	Regime mean bankfull depth/measured mean bankfull depth	[–]	Drat ^b

List A variables used to assign sediment regime following criteria in Table 2; List B were inputs to the Coarse SOM ($n = 193$).

List C were inputs to the Fine SOM ($n = 154$).

^a Normal distribution confirmed by Shapiro-Wilk test at $\alpha = 0.05$.

^b Or by histogram/normal quantile plot.

were used, relying on regional hydraulic geometry relationships (Jaquith and Kline, 2001, 2006) and pebble-count data from field assessments to provide an indication of sediment transport capacity (Supplementary text S1).

3.2. Assignment of sediment regime class

We assigned one of six sediment regime classes (Table 2, Fig. 2) to each study reach to describe the present regime for transport of coarse and fine (<63 μ m) fluvial sediment based on a combination of

geomorphic metrics and observations (Kline, 2010). The sediment regime classes lie on a continuum from supply-limited to transport-limited (Montgomery and Buffington, 1997); and classification focuses on processes operating at a temporal scale of 1 to 2 years, since classification metrics include dimensions (e.g., width, depth) relative to the bankfull stage, defined as the discharge with an approximate recurrence interval of 1.5 years, or Q1.5 (Leopold, 1994).

This classification scheme (Fig. 2) considers both the vertical and lateral dimensions of sediment (dis)connectivity in the context of varying degrees of channel confinement by valley walls (hillslope-channel

Table 2
Geomorphic characteristics of sediment regime classes.

Class	Transport (TR)	Confined Source and Transport (CST)	Unconfined Source and Transport (UST)	Fine Source and Transport/Coarse Deposition (FSTCD)	Coarse Equilibrium/ Fine Deposition (CEFD)	Deposition (DEP)
Color Key						
Valley Confinement	< 6	< 6	≥ 4	≥ 4	≥ 4	≥ 6
Slope	> 2 %	> 2%	< 4%	< 2%	< 2%	< 2% typically; > 2% occasionally
Incision Ratio (IR)	< 1.3	≥ 1.3	≥ 1.3	≥ 1.3	< 1.3	< 1.3
Entrenchment Ratio (+/- 0.2)	< 1.4 1.4–2.2 (B)	> 2.2	> 2.2 1.4–2.2 (B)	> 2.2 1.4–2.2 (B)	> 2.2	> 2.2
Width/Depth Ratio (+/- 2)	< 12 (A, G) > 12 (B, F)	< 12 (A, G) > 12 (B, F)	< 30 < 12 (E)	> 30 > 12 (E); > 40 (D)	< 30 < 12 (E); < 40 (D)	> 30 (> 40, alluvial fan)
Common Channel Evolution Stage †	I, V	II, III, IV	II, III	II, III, IV	I, V	
Rosgen (1996) Stream Type	A, B, G, F	A, B	G, F, B, E, C, Bc	E, C, Bc, F, D	C, E, D	C, D, Ca, Cb
Median Grain Size (D50)	bedrock, boulder, cobble, (occas. gravel)	cobble, gravel, sand	cobble, gravel, sand	cobble, gravel, sand	cobble, gravel, sand, silt	cobble, gravel, (occas. boulder)
Common Bedforms	cascade, step-pool	cascade, step-pool, plane bed	step-pool, plane bed, riffle-pool	riffle-pool	riffle-pool, dune-ripple	braided
Planform	single-thread linear to sinuous imparted by bedrock structure	single-thread linear to sinuous imparted by bedrock or encroachments	single-thread	single-thread meandering, localized bifurcations	single-thread, meandering	multiple-thread, braided
Type	Bedrock, mixed	mixed	mixed	Alluvial	alluvial	alluvial

† Channel evolution stage after Schumm et al. (1984) – see Supplementary.

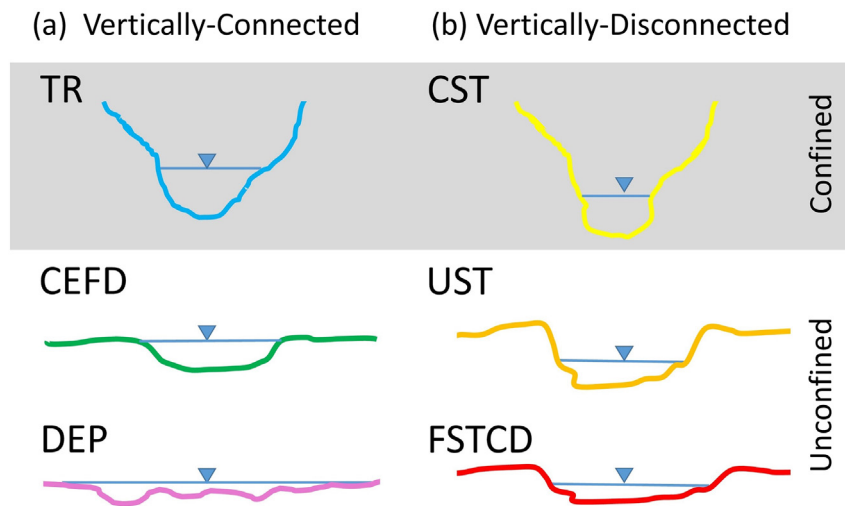


Fig. 2. Schematic of typical cross section for six sediment regime classes. Horizontal blue line depicts water surface of $Q_{1.5}$ discharge. Class abbreviations and color scheme are identified in Table 2.

coupling in highly-confined to semi-confined settings) and the vertical-lateral connectivity to floodplain (floodplain-channel coupling in unconfined settings). Three of the six sediment regime classes describe channels that are vertically connected – i.e., not degraded appreciably below their floodplain (incision ratio $IR < 1.3$), although the floodplain itself may be quite limited in areal extent (Fig. 2a); the other three classes are vertically-disconnected from the floodplain ($IR \geq 1.3$; Fig. 2b). The timescale of degradation processes resulting in loss of floodplain connection may be highly variable. Our assessment methods did not include a determination of incision timing beyond a subjective classification of active, historic or post-glacial.

In order from minor to major degree of lateral adjustment, representing bedrock-dominated to alluvial channel types, the three vertically-connected sediment regime classes (Fig. 2a) are:

- **Transport (TR)** reaches are confined- to semi-confined by their valley walls ($VC < 6$) and are supply-limited due to resistant channel boundaries and the relatively steep gradient ($>2\%$). TR reaches are not considered a significant source of coarse and fine sediments due to the high erosion resistance offered by the typical bedrock boundaries. Planform is controlled by the underlying bedrock structure, and floodplain areas for sediment storage are typically limited and discontinuous in areal extent (Wohl, 2010).
- **Coarse Equilibrium and Fine Deposition (CEFD)** reaches comprise self-formed (fully mobile) alluvial channels located in unconfined valley settings with low- to moderate-gradient ($<2\%$; riffle-pool and dune-ripple bedforms, occasionally plane bed). These channels are not incised ($IR < 1.3$), and therefore deposit fine sediments (suspended load) in their floodplains during floods of ≥ 2 –5-year RI. A coarse-sediment quasi-equilibrium condition is inferred from the condition over time of no net change in meander belt width, profile and average channel dimensions.
- **Deposition (DEP)** reaches are generally unconfined ($VC > 6$) and of lesser gradient ($<2\%$) but may have moderate to steep slopes (2% to 6%), e.g., Rosgen Ca or Cb stream types. Often DEP reaches are located immediately downstream of a steeper and more confined reach, and therefore represent locations of increased deposition and lateral migration due to the decreased stream competence imparted by the transition in valley topography (e.g., alluvial fans).

The remaining three classes (Table 2, Fig. 2b) represent channel reaches that exhibit a moderate to major degree of floodplain disconnection ($IR \geq 1.3$), resulting from either natural or human-induced

conditions, or both. Consequently, the channel becomes entrenched below an abandoned floodplain or terrace of glacial origin. Presented in order of increasing degree of lateral adjustment:

- **Confined Source and Transport (CST)** reaches exist in semi-confined to confined settings (higher degree of hillslope-channel coupling) of moderate to steep gradient and have more erosion-prone boundary conditions than TR reaches.
- **Unconfined Source and Transport (UST)** reaches occupy partly confined (by encroachment and channelization) to unconfined valley settings of moderate to low gradient ($<4\%$) and are characterized by a moderate to high degree of vertical separation from the floodplain ($1.5 < IR < 4$). By virtue of this incision, the sediment regime has shifted from a deposition-dominated condition to a transport-dominated condition (channel evolution stage II or early III). Width/depth ratios are generally small but variable.
- **Fine Source and Transport and Coarse Deposition (FSTCD)** reaches are located in unconfined valley settings of low gradient ($<2\%$) and are moderately to substantially incised ($IR > 1.3$). They are dominated by lateral adjustment processes including widening, planform adjustment accompanied by aggradation, typically in channel evolution stage III or IV.

Once reaches were classified into one of the above sediment regimes, assessment variables were examined to discern which ones had statistical power to differentiate between expert-assigned sediment regime classes using One-way Analysis of Variance (ANOVA) followed by Tukey Honest Significant Differences (HSD) tests between individual group means. For those variables (or their transformations) that were not normally distributed, nonparametric methods were applied (Kruskal-Wallis).

3.3. Pre-processing input data for SOM training

Reach-scale geomorphic and hydraulic metrics were explored using conventional statistical methods (e.g., Pearson or Spearman Rank correlations and Principal Components Analysis [PCA]) to select the SOM inputs (Lists B and C in Table 1). Variables that were very closely correlated to each other (i.e., Pearson correlation > 0.80) or which had little power to explain variance by PCA were dropped as inputs to the SOM. Data were also examined to help determine the appropriate SOM lattice configuration and size. A PCA was run on transformed variables, following the heuristic of Cereghino and Park (2009) that the

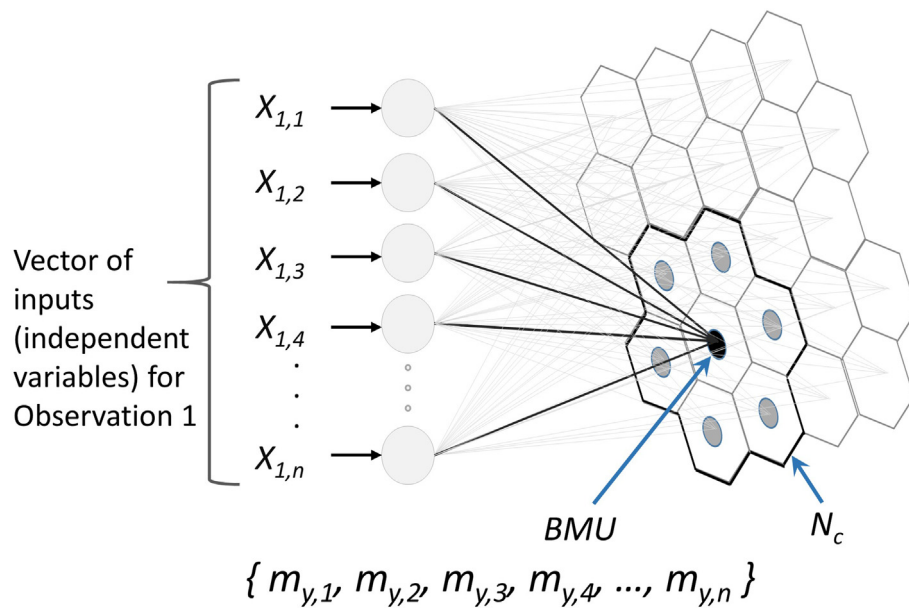


Fig. 3. Architecture of Self-Organizing Map illustrating the competitive algorithm (after Kohonen, 2001). Weights of the best matching unit (BMU) and lattice nodes within a user-specified neighborhood (N_c) surrounding the BMU are updated to make them slightly closer to values of the input vector.

optimal lattice column-to-row ratio approximates the ratio of the first two principal components. Statistical tests were performed in JMP (v. 12.0, SAS Institute, Cary, North Carolina).

3.4. Clustering algorithm

We clustered our reaches using an unsupervised algorithm – a Self-Organizing Map (SOM; Kohonen, 2001); the data set has p observations of n independent variables. The “unsupervised” descriptor means that data were presented to the clustering algorithm without their expert-assigned sediment regime classifications, and without a predetermined number of outcome clusters (i.e., sediment regime classes). Like conventional clustering techniques that are also data-driven (e.g., k-means and unsupervised hierarchical clustering), the SOM will aggregate p observations into k groups, each with internally similar values for the n independent variables. However, certain features unique to the SOM technique (described below) ensure that clustering proceeds in a manner that is more robust to outliers, non-continuous data types, and data that are not normally distributed (e.g., the latter two conditions would violate underlying assumptions of traditional clustering techniques). Similar to traditional methods such as PCA, regression trees, and logistic regression, the SOM is useful for reducing the dimensionality of data and for selecting variables that strongly influence clustering or classification (i.e., feature selection). Yet, the SOM has advantages over these traditional methods for exploratory data analysis and visualization (Eshghi et al., 2011).

The SOM reduces a multidimensional data space to a lower-dimensional space, typically a 2-D plane or lattice having a number of individual nodes, also called a Kohonen feature map (Kohonen, 2013). The outcome of a converged lattice is such that observations introduced to the SOM self-organize into “a kind of similarity diagram” (Kohonen, 2013) where similar observations will cluster and be mapped to a similar location on the lattice/map. Each of the input variables may also be viewed on the converged lattice in what is known as a “component plane”, where values of the input variables can be observed with their associated cluster.

Typically, the SOM input data are normalized so that variables of higher magnitude do not overly dominate the clustering process. Our variables were each range-normalized to a value between 0 and 1 before beginning SOM training (Alvarez-Guerra et al., 2008):

$$\text{norm}(x_i) = \frac{x_i - \min(x_i)}{\max(x_i) - \min(x_i)}.$$

A hexagonal lattice topology (Fig. 3) was selected, given the potential for conditional bias between input variables (Kohonen, 2001). At the initial state of the lattice, each node is assigned a vector, \mathbf{m} , of random values (i.e., weights) ranging from 0 to 1; the vector length is equal to the number of input variables, n . One of the p observations is then selected at random from the data set, and its vector \mathbf{X} of n variables $\{X_{p,1}, X_{p,2}, X_{p,3}, \dots, X_{p,n}\}$ is presented to the vector of weight values $\{m_{y,1}, m_{y,2}, m_{y,3}, m_{y,4}, \dots, m_{y,n}\}$ in each lattice node, y . The distance, or dissimilarity, between the observation vector and each weight vector for each lattice node (y_1, y_2, \dots, y_Y) is computed. Euclidean distance is commonly used (Kohonen, 2013), and was also used in this study. The SOM uses a competitive (“winner-takes-all”) algorithm to ensure that the selected node has a weight vector that is most similar to the observation vector. The weights of this Best Matching Unit (BMU), along with a user-defined neighborhood of nodes (N_c) around the BMU, are incrementally adjusted to be more similar to the input vector. This user-defined neighborhood of nodes is one of the features that distinguishes the SOM from other more common methods of clustering, such as k-means (which only updates weights of a single node).

The weights of the BMU and neighborhood units are adjusted gradually by a distance that amounts to a small fraction of the total distance between the input vector and each weight vector. This fractional distance is applied in accordance with a user-specified learning rate parameter. A next observation vector is then selected at random from the data set and compared to the weight vectors of each lattice node; a BMU is identified, and its weights and that of its neighbor nodes are adjusted, as the process is repeated in each successive iteration. Commonly, both the size of the updating neighborhood and the learning rate are decreased linearly with progressive iterations, moving from a coarse to fine tuning process. Over multiple iterations, the lattice weights are adjusted by smaller amounts and the algorithm converges (self-organizes). At convergence, the adjusted weight vectors will more closely reflect the input vectors and will be arranged across the lattice such that similar stream reach observations are aggregated together. The distance (or dissimilarity) between weight vectors at convergence is then examined to define clusters of nodes containing similar weights. Several methods are available; often hierarchical clustering is used (Vesanto and Alhoniemi, 2000) as was the case in this

study. The SOM algorithm was implemented in the R programming language (R Core Team, 2017) applying the “kohonen” package (Wehrens and Buydens, 2007, v. 3.0.2 released 2017).

3.5. SOM computation, training and cluster validation

SOM training was performed in 900 iterations. The learning rate was set initially at 0.05 and decreased linearly to 0.01. The neighborhood size decreased linearly from a radius encompassing two-thirds of the lattice, to a value of 0 at one-third of the iterations - at which point, the algorithm was only updating the BMU (analogous to k-means clustering).

For a given data set, several multi-iteration SOM runs were performed utilizing lattices with varying configurations and numbers of nodes. Column-to-row configurations were chosen to closely approximate the ratio of the first two principal components of the transformed variables (Cereghino and Park, 2009). As an additional constraint, the final grid size (Y nodes) approximated a value of $5\sqrt{Y}$ following the heuristic of Vesanto et al. (2000), yet did not exceed the number of input variables. For each converged lattice configuration, clusters of similar weights were identified using hierarchical clustering specifying k groups, where $k = \{3, 4, \dots, 8\}$. We identified the “optimal” number of clusters for a given input data set by examining cluster separation and compactness of clusters to maximize a nonparametric F statistic (Anderson, 2001), computed as the ratio of between-cluster to within-cluster variance. At the same time, we identified the number and configuration of lattice nodes with best resolution to achieve a local minimization of quantization error (Kohonen, 2001; Cereghino and Park, 2009). Calculation of the nonparametric F statistic was aided by the “adonis” function in the “vegan” package in R (Oksanen et al., 2017).

Clusters were also examined post hoc to further understand variables driving the clustering. For each input variable, the intra-cluster mean (on a normalized scale) was plotted against the overall mean, and the magnitude and direction relative to the overall mean were examined. While traditional statistical methods (see Section 3.2) largely guided which geomorphic and hydraulic variables were used as inputs to the SOM, these variable plots by cluster and the component plane for each variable were examined to further refine a parsimonious list of input variables.

4. Results

Our results are organized to first summarize the geomorphic condition of the 193 assessed reaches. We then describe the expert-assigned sediment regime classes and review those geomorphic metrics with most power to predict class membership. Finally, we summarize the clustering outcomes from the SOM, performed in two stages, and highlight the ability of this nonlinear algorithm to replicate expert-assigned classifications.

4.1. Geomorphic condition

Bedforms most commonly encountered in the 193 study reaches included step-pool, plane bed, riffle-pool and dune-ripple (Fig. 4a). Riffle-pool and dune-ripple bedforms were associated with channel gradients less than 2% in unconfined valley settings. Our data set included fewer occurrences of bedrock, cascade and braided bedforms (Fig. 4b). In general, the assessed reaches transitioned from confined headwaters to unconfined downstream valley settings (Fig. S1). However, a stepped longitudinal profile was evident for many streams due to the influence of exposed bedrock knickpoints that typically coincided with valley pinch points. Example longitudinal profiles of study area streams and tributaries indicate the typical sequencing of stream types from upstream to downstream and the relative location of more macro-scale

features including bedrock knick points and glacial and post-glacial landforms including glaciolacustrine or glaciofluvial terraces and alluvial fans (Fig. 4c, d, e, f).

4.2. Sediment regime classification by experts

Sediment regimes assigned to the 193 study reaches by the investigators included representatives from each of the six categories (Fig. 4b). Thirty-five (18%) of the assessed reaches were in confined settings (TR, CST), while the remaining reaches (158; 82%) were in naturally-unconfined settings. The expert-assigned classifications were occasionally somewhat subjective, particularly where classification rules overlapped. Stream assessment protocols allow for some variation in the threshold values of Entrenchment Ratio and Width/Depth Ratio that define sediment regime classes. The threshold value for Entrenchment Ratio can vary by ± 0.2 units, and the threshold value for Width/Depth ratio can vary by ± 2 units (Table 2). Given the uncertainty associated with channel-floodplain measurements, and the “scaling up” of measurements collected at the cross-section scale to represent the reach scale, a few reaches did not easily conform to all of the rules for a given sediment regime class, and instead spanned two classes, requiring domain experts to make a final determination of class membership.

4.2.1. Confined reaches

Valley confinement (VC; Fig. 5a) and Entrenchment Ratio (ER; Fig. 5b) generally had power to distinguish confined reaches in TR and CST classes from the unconfined sediment regimes (ANOVA/Tukey HSD on log-transformed values, $p < 0.05$), with the exception that their mean ER values were not significantly different from that of UST reaches ($p = 0.12$ and $p = 0.49$, respectively). The confined reaches (TR, CST) were generally found in steeper settings ($>2\%$) and most often in the case of TR were co-located with bedrock gorges (e.g., Fig. 4e). However, a few reaches of gradient $<2\%$ were classified in either TR (12 of 25) or CST (2 of 10) where bedrock boundary conditions controlled the confinement at a mid-valley pinch point (i.e., VC ratio less than 1, Fig. S2e). The Specific Stream Power balance (SSP_{bal}) distinguished TR reaches from the unconfined sediment regime classes (ANOVA/Tukey HSD on log-transformed values, $p < 0.0001$). However, means were not significantly different in pairwise comparisons between the other classes ($p > 0.10$; Fig. 5f).

CST reaches were themselves distinguished from TR reaches by Incision Ratio, which reflected a significantly higher degree of vertical disconnection for this class ($p < 0.001$). Additionally, SSP_{bal} had some power ($p = 0.02$) to distinguish CST from TR reaches. We infer that both fine and coarse sediment fractions are exported through reaches in these TR and CST classes. Elevated values of SSP (Fig. 5e) would support this interpretation, although it would take a flood event greater in magnitude than the Q1.5 to exceed the critical SSP required to mobilize the D85 particles or larger, as suggested by the SSP_{cr} ratio (Fig. S2u). Due to the somewhat incised status of CST reaches and more erodible boundary conditions (i.e., not consistently bedrock), reaches in this class can be a source as well as a transporter of coarse and fine sediments. Close-coupling to hillslopes can lead to lateral inputs of sediment and large woody debris, but our CST reaches exhibited varying degrees of valley confinement, and thus hillslope coupling (Fig. S2d), with some but not all characterized by mass wasting from either glacial till or glaciolacustrine sediment sources (Fig. 4c, d, e, f).

4.2.2. Unconfined reaches

Unconfined reaches in CEFD, UST and FSTCD classes had significantly higher valley- to bankfull-width ratios than their confined reach counterparts (Fig. 5a), and occupied lower-gradient valley settings (Fig. S2g) that within our study area were underlain by a mix of glaciolacustrine, glaciofluvial, post-glacial fluvial and glacial till parent materials (Fig. 4). The VC ratio (subject reach to upstream reach VC) was generally above 1 for these unconfined classes, reflecting the

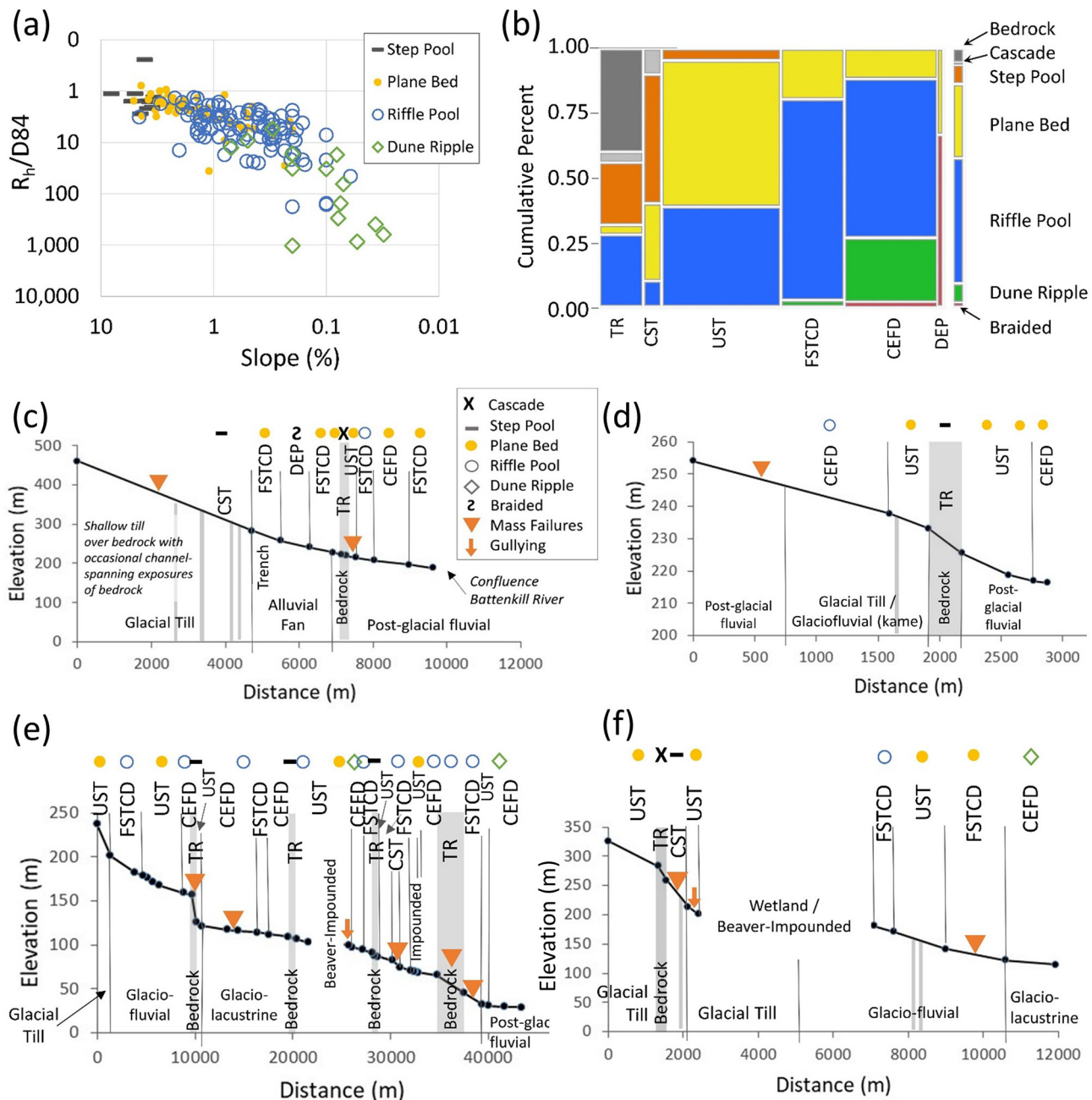


Fig. 4. Distribution of bedforms by: (a) slope – relative roughness plot; and (b) sediment regime class ($n = 193$). Braided ($n = 3$) bedrock ($n = 10$) and cascade ($n = 2$) bedforms omitted from panel a. Column widths in panel b vary by sample size. Longitudinal profile of reach classifications for (c) Roaring Branch (Battenkill), (d) Fayville Branch (Battenkill), (e) Lewis Creek and (f) Hollow Brook (Lewis). Map locations of these streams are included in Supplementary Fig. S1.

prevalence of increasing valley and channel widths with downstream distance. However, some reaches had values below 1, indicative of longitudinal variability and discontinuities imparted by bedrock and glacial deposits (Fig. S2e).

CEFD reaches were distinguished from UST and FSTCD reaches by statistically-higher mean values for ER and lower values of IR ($p < 0.001$; Fig. 5b, c, respectively). These low-gradient reaches were well-connected to their floodplains and characterized by finer-grained bed sediments (Fig. S2h) that were generally well-sorted (i.e., low $D84-D16$ differential, Fig. S2i). High values for the $R_h/D84$ ratio in CEFD reaches reflect these smaller grain sizes, as well as the generally higher hydraulic radius values characteristic of sinuous channels with dune-ripple bedforms (Fig. 4a) that comprise a subset of reaches in this class (Fig. 4b). Mean SSP values for the CEFD class were lower than

the UST or FSTCD classes ($p < 0.001$). The unconfined, well-connected CEFD reaches exhibited a mean and median SSP of 41 and 34 $W m^{-2}$, respectively, with an interquartile range from 16 to 55 $W m^{-2}$ (Fig. 5e). The median and mean SSP_{bal} values were below 1, suggesting deposition-dominated conditions. For reaches in this CEFD class, we infer quasi-equilibrium transport of coarse sediment from the condition of near-regime values for channel dimensions (Fig. S2p, q) and meander belt width (not presented). Fine-sediment (suspended load) deposition in the connected floodplains is expected during overbank floods which would correspond to a recurrence interval ≥ 1.5 years due to the low incision ratios (Fig. 5c).

UST and FSTCD reaches on the other hand were vertically disconnected from their floodplains ($IR \geq 1.3$; Fig. 5c). Reaches in both classes had statistically greater mean SSP values than CEFD reaches

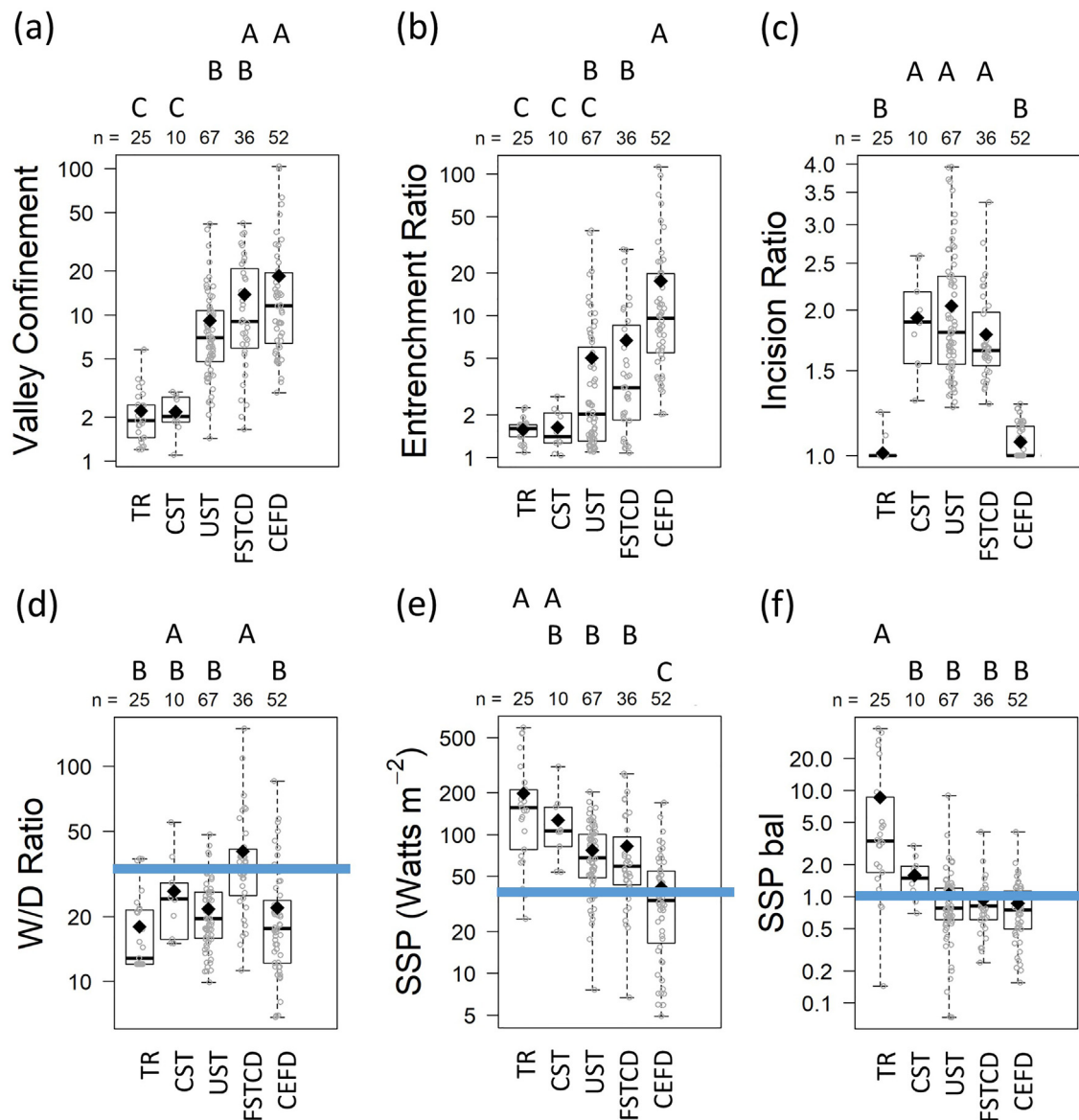


Fig. 5. Box plots displaying range and central tendency of geomorphic and hydraulic variables by assigned sediment regime class. Solid, black horizontal lines depict median values; black diamonds depict arithmetic mean of non-transformed values. Blue horizontal lines depict threshold values discussed in the text. Unique letters indicate statistically-significant differences between class means by ANOVA/Tukey HSD on transformed variables ($\alpha = 0.05$). See Supplementary for details.

($p < 0.0001$; Fig. 5e). Yet the two classes were distinguished from each other by their W/D ratios ($p < 0.0001$; Fig. 5d), due to differences in boundary resistance to erosion. UST reaches were more likely to have artificial armoring (Fig. S2m) and exhibited greater percentages of channel straightening (Fig. S2y), associated with a higher degree of floodplain encroachment by roads and development. Along with human-constructed features (e.g., bank armoring or road embankments), various natural features of these channels (e.g., presence of woody riparian buffers, cohesive channel bed and bank sediments, lateral exposures of bedrock) may have also formed resistant channel-boundary conditions. Where channel boundaries are not stabilized by armoring or vegetation, we infer both fine and coarse sediment fractions are sourced and exported through UST reaches due to enhanced stream bed and bank scour imparted by the incised and entrenched cross section.

Due to lower boundary resistance, FSTCD reaches had significantly higher width/depth ratios than UST (or CEFD) reaches ($p < 0.0001$; Fig. 5d). FSTCD reaches were also characterized by a higher degree of coarse sediment deposition than UST reaches (Fig. S2n), greater

numbers of flood chutes (Fig. S2o) and riffle cross sections that were wider and shallower than regime (Fig. S2p, q). We infer net deposition of coarse sediments in these reaches due to reduced stream competence in the wide and shallow cross section; yet, the incised and entrenched status of that cross section relative to the surrounding floodplain means that fine sediments will continue to be sourced from lateral bank migration and transported to downstream reaches.

The DEP class had a small sample size in the studied reaches ($n = 3$; 1.6%), and therefore is not represented in Fig. 5; this is a typical representation for this class in Vermont, based on field experience of the investigators. One DEP reach was located at the transition from a 4th-order channel to a downstream reservoir delta; the remaining two reaches were located in alluvial fan settings (e.g., Fig. 4c).

4.3. Clustering outcomes

To determine whether the above expert-assigned sediment regime classes could be replicated by a data-driven, unsupervised clustering

algorithm, we introduced a variety of geomorphic and hydraulic variables to the SOM, but withheld the above class assignments. A two-stage implementation of clustering was warranted to control for different scales of classification - essentially, a coarse-tuning SOM for all 193 reaches ranging in character from steep bedrock channels to alluvial channels, followed by a fine-tuning SOM applied to the subset of 154 reaches comprising unconfined, low-gradient ($<2\%$), self-formed alluvial channels. The coarse-tune SOM was trained using largely reach-scale geomorphic variables, while the fine-tune SOM was trained by adding cross-section-scale hydraulic variables that reflect stream competence as affected by channel-floodplain configurations.

4.3.1. Coarse-tune SOM

The coarse-tune SOM was trained using List B of input variables (Table 1). These input data self-organized into seven clusters, broadly corresponding to our six sediment regime classifications (Table 2). The multivariate input data for the 193 training reaches were reduced to a two-dimensional 6×13 lattice for visualization (Fig. 6a). The column-to-row ratio for this lattice (2.2) approximated the ratio (4.6/1.9) of the first two principal components of the (transformed) input data. The multivariate reach observations self-organized on the SOM lattice during training, such that reaches with similar variable sets aggregated together; and logical groupings of these observations were partitioned into seven clusters. To illustrate an advantage of the SOM over other multivariate statistical techniques for pattern visualization, component planes for a select number of the SOM input variables are provided in Fig. 6b (see also Fig. S3). Each input variable may be superimposed on the converged SOM lattice to generate a “component plane”, where the range-normalized values vary in magnitude across the lattice. For example, reach observations that aggregated to Cluster 4 in the upper-left corner of the lattice, are characterized by high values of slope relative to other observations, as illustrated by the warmer tones in that region of the component plane for slope. These are also vertically-stable reaches, as suggested by the low values (cool tones) in the same region of the component plane for IR. Reach observations

that aggregated to Cluster 7 of the SOM lattice are also vertically-stable (low values for IR), but are characterized by low slope values, and higher values than other reaches for VC and ER.

Bar plots of intra-cluster means (on a normalized scale) relative to overall means for each parameter suggest which variables are important in defining the sediment regime clusters (Fig. 7a). Two TR clusters (4 and 5) comprised vertically-stable reaches confined by valley walls (Fig. 7a). These reaches were characterized by steeper-than-average slopes, greater-than-average SSP, and coarser bedload (dominated by bedrock in each case). Cluster 5 reaches were distinguished from Cluster 4 by a high SSP_{bal} value (>1 ; see Supplementary data). While this condition might suggest the propensity for incision, the bedrock boundary conditions would be expected to offer resistance in the present hydrologic regime. Therefore, in this data set ($n = 193$) and our study area (which includes reaches from a range of topographic settings), SSP_{bal} is a variable with ability to discern bedrock-controlled knickpoints at a transition from a lesser-gradient upstream reach.

At the opposite end of the sediment transport continuum, representing transport-limited conditions, two clusters (6 and 7) in unconfined settings were characterized by larger-than-average VC and ER values (Fig. 7b). Cluster 6 (DEP) reaches comprise coarser-than-average bedload and very high W/D ratios (braided channels). Cluster 7 (CEFD) reaches, however, were distinguished by their lower-than-average W/D ratios, lesser slopes and finer-grained bed material. These reaches were further characterized by a marked transition to a much more open valley setting compared to the upstream reach (i.e., high VC ratio). In our study region, Cluster 7 reaches were located along the edge of post-glacial Lake Vermont, a higher-stage pre-cursor to Lake Champlain (Stewart and MacClintock, 1969), and channel boundaries were composed of cohesive glaciolacustrine silts and silty-sands with varying percentages of clay (dune-ripple bedforms).

The remaining reach observations in this coarse-tune SOM aggregated to three clusters of vertically-disconnected reaches in unconfined settings (Fig. 7c). In general, Class 1 contained reaches associated with a higher-than-average IR, lower-than-average ER and coarser-grained,

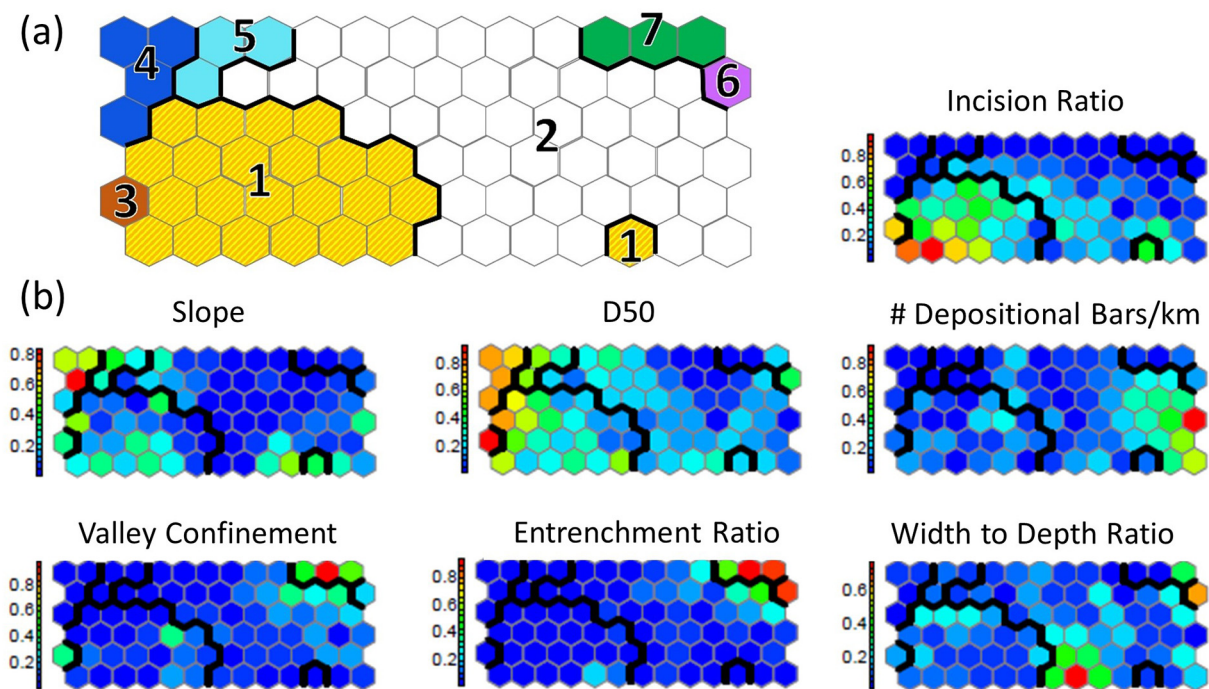


Fig. 6. Coarse-tune SOM clustering of study area reaches, including (a) converged SOM lattice showing clusters; and (b) component planes for selected input variables, in which the color scheme represents a “heat map” grading from low (cool blue tones) to high (warmer red tones) range-normalized values for each independent variable. Component planes for additional variables are presented in Supplementary Fig. S2.

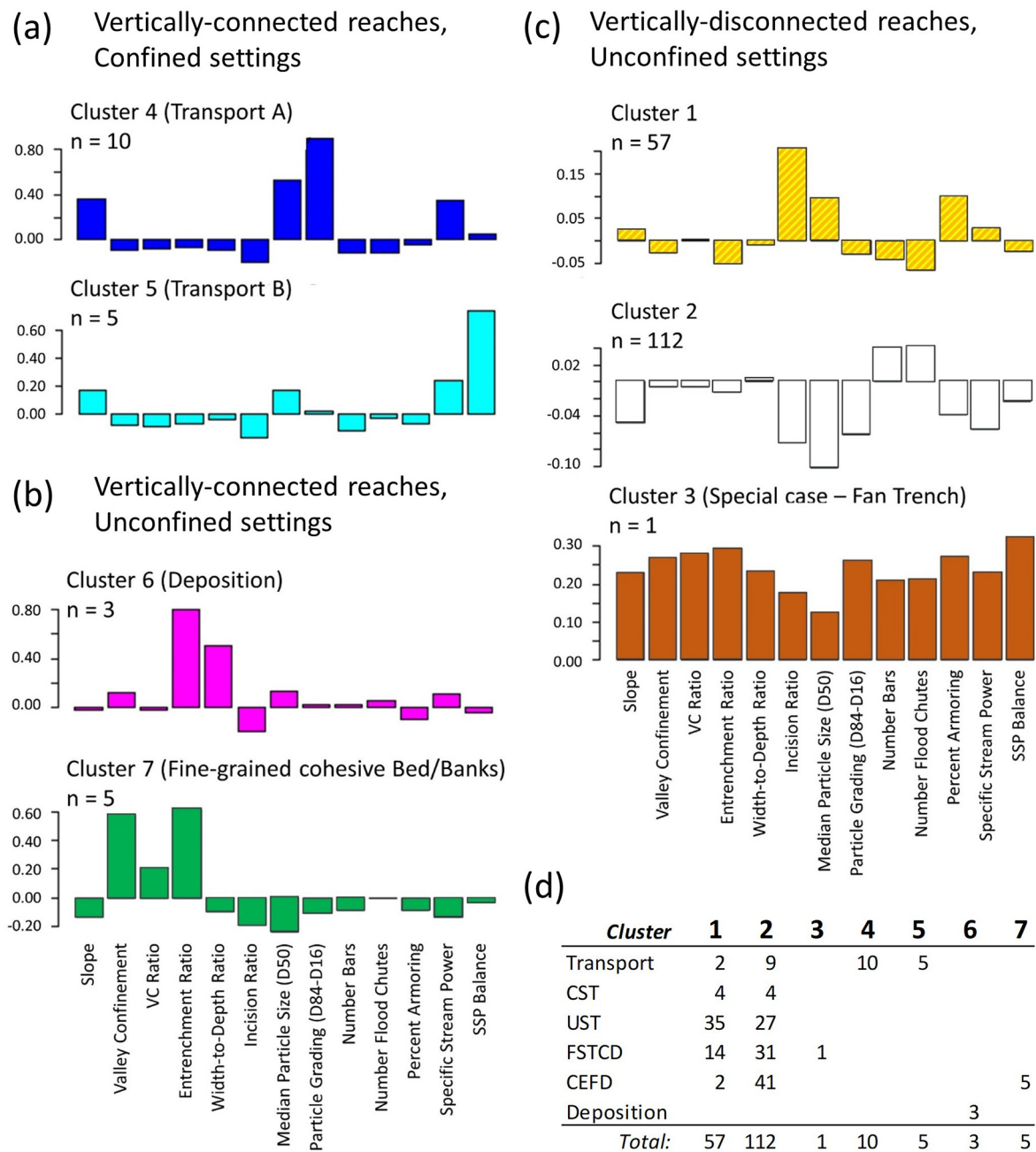


Fig. 7. Coarse-tune SOM clustering of study area reaches, including (a) vertically-stable reaches in confined settings, Clusters 4 and 5; (b) vertically-stable reaches in unconfined settings, Clusters 6 and 7; (c) vertically-disconnected reaches in unconfined settings, Clusters 1, 2 and 3 (n = number of reaches per cluster; y-axis represents range-normalized values); (d) summary of expert-assigned sediment regimes by cluster. Color scheme of bar plots corresponds to cluster colors in Fig. 6a.

well-graded, bed material. Class 2 reaches, however, were much less incised (on average), and exhibited higher ER values, lower slopes, and finer-grained, well-sorted, bed materials. Variables including number of depositional bars, number of flood chutes, percent armoring, and SSP were useful in distinguishing between Clusters 1 and 2, as the cluster means for these factors trended in opposite directions from the overall average.

To evaluate the utility of the coarse-tune SOM for partitioning reaches into sediment regimes, we have summarized by cluster (Fig. 7d) the sediment regime classifications assigned to reach observations in Section 4.2. We have also overlaid reach observation numbers on the lattice nodes to which they clustered, color-coded by the

assigned sediment regime classification (Fig. 8). Based on 13 independent variables (list B in Table 1), the coarse-tune SOM was able to distinguish reasonably well between sediment regimes at the extremes of the lateral-confinement continuum for vertically-stable reaches (Fig. 8a). Clusters 4 and 5 are two variations of the TR regime, with the latter representing local knickpoints. Cluster 6 contains the DEP reaches, while Cluster 7 represents a subset of the CEFD classification comprised of fine-grained, cohesive channel types. Thus, along the lattice-horizontal dimension, the reach observations have self-organized into a configuration that is suggestive of the continuum of reach types from supply-limited to transport-limited (left to right in Fig. 8), as proposed by Montgomery and Buffington (1997). Along the lattice-vertical

dimension, an increasing gradient of vertical disconnection from the floodplain is evident (Fig. 8b). An increasing degree of channel or catchment stressors may also be suggested by the distribution of parameter values that can be visualized on the component planes for IR, ER, percent armoring, and numbers of depositional bars and flood chutes (Fig. S3).

Reaches in Clusters 1 and 2, on the other hand, each have a mix of expert-assigned sediment regimes (Fig. 7d), although the former is dominantly represented by UST, and the latter by CEFD regimes. Thus, governing variables used in the coarse-tune SOM may have only moderate power to discern between sediment regimes, particularly in the context of the full range of stream types from bedrock-cascade to silt-dune-ripple channels. Therefore, a second fine-tune SOM was applied to cluster observations from only the unconfined, low-gradient (<2%), self-formed alluvial channels.

4.3.2. Fine-tune SOM

The fine-tune SOM was trained on the subset of 154 reach observations consisting of both geomorphic and hydraulic input variables (list C of Table 1). These reaches were unconfined, low-gradient (<2%) channels predominantly alluvial in nature, although characterized by the occasional bedrock grade controls or valley pinch points. Multivariate ($p = 10$) input data for the 154 training reaches were reduced to a two-dimensional 6×12 lattice, with a column-to-row ratio (2.0) similar to the ratio of the first two principal components of the (transformed) input data (4.1/2.2). Non-transformed, but range-normalized, input data mapped to three clusters (Fig. 9a) that are characterized by different combinations of input variables (Fig. 9b).

The fine-tune SOM has closely replicated the expert-assigned sediment regimes (Fig. 9c), and performed better than the coarse-tune SOM for these unconfined CEFD, UST and FSTCD classes. Variable plots (Fig. 9b) illustrate that CEFD (Cluster 1) reaches were differentiated from the other two classes, principally by their lower-than-average IR

(<1.3), and lower slopes and SSP. The FSTCD (Cluster 3) reaches were discerned from their UST counterparts (Cluster 2), by elevated values for width ratio and W/D ratio, a higher incidence of flood chutes, and lower-than-average mean depth ratio, reflecting the “wide-and-shallow” nature of these channels. If the expert-assigned regimes are taken as “correct”, the fine-tune SOM resulted in a correct classification rate of 64%, overall, with slightly higher classification rates for UST and CEFD classes (66% and 65%, respectively) than the FSTCD class (60%).

5. Discussion

5.1. SOM refinement of sediment regime classifications

Multivariate stream geomorphic assessment data for 193 Vermont stream reaches self-organized into seven clusters (sediment regimes) that broadly replicated and refined six classifications offered in a VT Agency of Natural Resources River Corridor Planning Guide utilized for river management (Kline, 2010). These sediment regimes are a function of both geomorphic and hydraulic variables operating at the cross-section scale (e.g., relative roughness, depth) and reach-scale (e.g., valley confinement, slope). While these metrics are based largely on observations of form, the assigned sediment regimes reflect the spatial and temporal context of multiple historic and active processes that have manifested the present channel and floodplain configuration (Wohl, 2018). These sediment regime classes could be considered as fluvial process domains of Montgomery (1999), or “spatially identifiable areas characterized by distinct suites of geomorphic processes”, if we extend this conceptual framework to define reach-scale patterns of sediment sourcing, deposition and transport dynamics. Our sediment regime classes are developed at a more granular scale than the process domains (glacial vs. fluvial) of Livers and Wohl (2015) defined for a study area undergoing active glaciation (Colorado Front Range of western US). Our study reaches are lower in elevation and would all

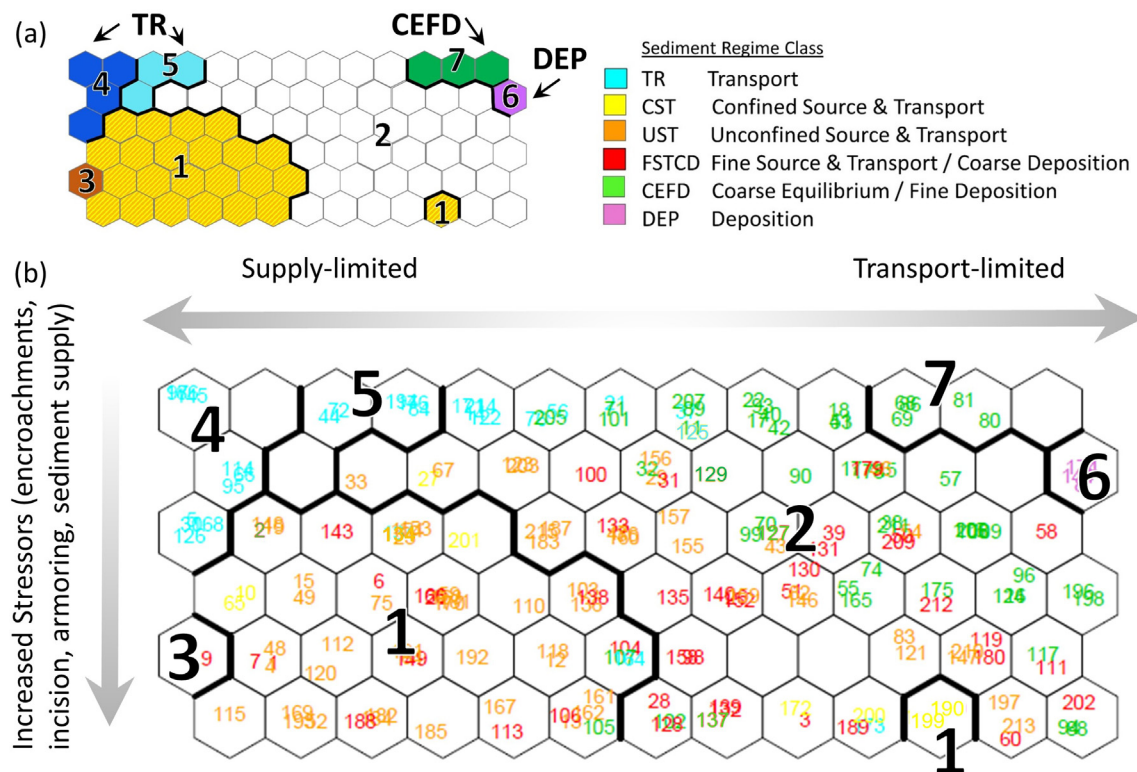


Fig. 8. Reach observation numbers (color-coded by expert-assigned sediment transport regime – see key above) plotted to SOM to visualize where observations clustered on the coarse-tune SOM.

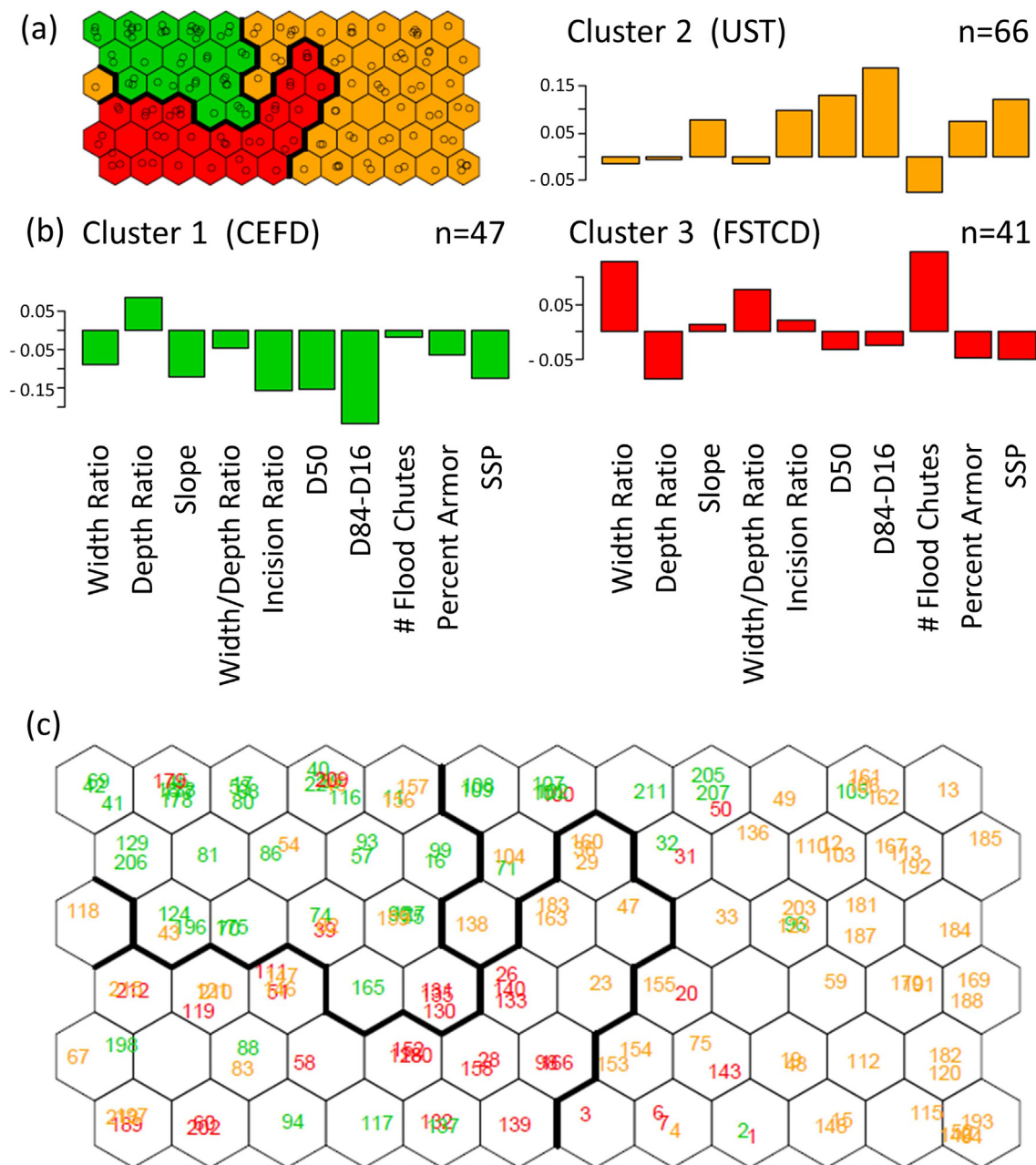


Fig. 9. Fine-tune SOM clustering of study area reaches, including (a) converged SOM lattice; (b) variable bar plots by cluster; and (c) reach observation numbers plotted to lattice, color-coded by expert-assigned sediment transport regime.

be classified as fluvial, but are influenced by former glacial activity. Multiple bedforms can occur in a given sediment regime (Fig. 4b). Downstream sequencing of these sediment regime classes and their associated bedforms is variable and influenced in part by the spatial and temporal context of macro-scale, glaciogenic landforms as well as periodic bedrock exposures that create a stepped longitudinal profile (Fig. 4c, d, e, f). In this sense, our results are consistent with findings from a mountainous region of coastal British Columbia with a similar glacial legacy. Brardinoni and Hassan (2007) applied multivariate discriminant analysis paired with PCA to channel and floodplain metrics for classification of process domains, and identified a variation on the idealized downstream continuum of stream types after Montgomery and Buffington (1997), related to the presence of glaciogenic landforms and varying degrees of hillslope-channel coupling. Their study considered relatively high-relief, undeveloped catchments of consistent land

use. In contrast, our lower-relief study catchments comprise a greater range of developed and agricultural uses (Table S1). Thus, the fluvial geomorphic condition of our Vermont reaches also reflects the impacts of historic and active channel and floodplain encroachments and disturbances (i.e., channelization, dredging, armoring, berming, gullyng) superimposed on inherited glacial landform effects.

Our sediment regimes comprise the full continuum of stream types proposed for mountain systems by Montgomery and Buffington (1997), excluding colluvial channels. Our results extend this framework, by considering the vertical disconnection of a channel from its floodplain resulting from a variety of natural and human disturbances. Similarly, Phillips and Desloges (2014b) identified channel entrenchment as a factor contributing to within-class variability among unconfined, alluvial channel types from a glacially-conditioned setting in southern Ontario. Channel incision in our study area may have occurred

over post-glacial to historic time frames during base-level lowering upon draining of high-elevation post-glacial lakes (Stewart and MacClintock, 1969) or as a result of human stressors channel manipulation (Kline and Cahoon, 2010), sediment-starved conditions downstream of historic mill dams (Magilligan et al., 2008) or watershed-scale stressors such as increased runoff from urbanization or deforestation (Booth, 1990). For several reaches, we inferred a complex history of degradation, with active or historic incision overprinted on post-glacial incision. Regardless of the cause, the present channel form and degree of vertical disconnection imparts varying sensitivities to future adjustment, and influences fine and coarse sediment production, transport and deposition.

Our nonlinear clustering algorithm appears reasonably robust to these complex and multivariate interactions and was able to identify unique sediment regimes for reaches comprising a range of channel types from confined to unconfined, steep- to shallow-gradient, mid-to-high order, and bedrock to alluvial channels types. To resolve differences between sediment regime classes, application of the SOM in two stages was required, each incorporating unique combinations of hydraulic and geomorphic variables. The coarse-tune SOM identified sediment regime classes at the supply-limited and transport-limited extremes of the continuum. Bedrock channels and confined, steep-gradient reaches were identified as transport-dominated reaches (TR). At the supply-dominated extreme, braided, depositional channels (DEP) were identified at alluvial fan or delta settings. The coarse-tune SOM also identified the unique case of an alluvial fan head trench (Schumm, 2005) that likely formed under post-glacial times related to base-level lowering as proglacial lakes impounding downstream reaches were drained (DeSimone, 2000).

CST reaches were less well defined by the coarse-tune SOM which may reflect the variable degrees of hillslope coupling noted in our reaches, consistent with findings of Brardinoni and Hassan (2006, 2007) in formerly-glaciated coastal British Columbia. This finding may also reflect temporal variability in sourcing of materials and the importance of episodic inputs from extreme events that recur on an interval exceeding the Q1.5 scale of our sediment regime. Evidence from the region (including some of the study area catchments) suggests that mass wasting processes from our coupled hillslopes (where they exist) may be most significant during low-frequency, high-magnitude flows (Dethier et al., 2016).

The second-stage, fine-tune SOM nuanced differences in sediment sourcing and transport for the alluvial, unconfined reaches, although it required sub-setting of the data to only the unconfined reaches and slight modification of input variables. In this sense, the SOM is similar to traditional statistical techniques used to cluster fluvial process regimes, where optimal performance requires pre-filtering by consistent land cover/land use (e.g., Brardinoni and Hassan, 2007) or valley setting. For example, Phillips and Desloges (2014b) used k-means clustering, PCA, and discriminant analysis of geomorphic parameters to identify four channel-floodplain types. Their analysis was constrained to low-gradient, single-thread channels in unconfined settings, corresponding generally to C3, C4, E5, and E6 stream types of Rosgen (1996).

The relatively low mean and median SSP (41 and 34 W m^{-2} , respectively) characterizing the vertically-connected and quasi-equilibrium state CEFD reaches of our study area are similar to stability thresholds identified by others in humid temperate regions. For catchments in the United Kingdom, Bizzi and Lerner (2013) identified an unconfined-channel stability threshold of 34 W m^{-2} separating erosion-dominated reaches from those in a quasi-equilibrium state. Brookes (1987) identified a similar threshold at 35 W m^{-2} marking a transition between erosion-dominated and deposition-dominated channels for study areas in Denmark and the United Kingdom. Our vertically-disconnected UST and FSTCD reaches exhibited SSP values in an interquartile range that exceeded this stability threshold, although this variable had limited power to distinguish between these two classes. It is important to note that our SSP values were generated from

regional hydraulic geometry relationships and would not necessarily reflect the influence of channel-floodplain manipulations that have persisted for UST reaches; rather, elevated SSP values would largely reflect the steeper gradients of the UST and FSTCD reaches as compared to CEFD reaches.

5.2. SOM advantages for addressing uncertainty in sediment regime classifications

Uncertainty will arise when attempting to classify the complex, non-linear dynamics of fluvial sediment regimes from large sets of independent variables, particularly when rule sets or models are inadequate to define threshold effects or multivariate interactions. Since there are no sharp boundaries (“edges”) between sediment regimes, these classifications reflect a continuum of change, both temporally and spatially. The nonlinear, unsupervised SOM has particular advantages over conventional and linear statistical techniques for addressing these uncertainties and highlighting the potential influence of variable spatial and temporal scales of assessment. The hierarchical nature of spatial scales in a catchment suggests that the channel-floodplain geometry measured at a cross section scale can be relied upon to infer processes characteristic of the reach scale (Frissell et al., 1986), provided the reach length is appropriately delineated to reflect relatively homogeneous characteristics. In this study, cross-section locations were chosen to be representative of the reach and not influenced by localized sources of instability, such as stream crossings. However, subjectivity in this choice may have introduced bias, and it is possible that select geomorphic or hydraulic parameters obtained at the cross section may reflect processes operating at a more granular scale than is characteristic of the reach as a whole (Lea and Legleiter, 2016). For example, channel aggradation upstream of large woody debris might locally skew the D50 or D84 minus D16 values captured at a cross section.

In this study, executing the SOM in two stages helped to address uncertainty introduced by different spatial scales of classification for our broad range of stream types (bedrock-cascade to silt-dune-ripple). Coarse SOM results for the lumped range of stream types, and List B input variables, indicate that certain sediment regimes are more predictable (e.g., TR, DEP), while remaining regimes have more uncertainty. The latter group may represent reaches closer to thresholds and “more vulnerable to small perturbations” (Phillips, 2003). Using only the subset of reach data from unconfined settings (i.e., controlling for valley confinement and slope), the fine-tune SOM and a slightly different set of input variables (List C) were better able to differentiate between sediment regime classes.

Another source of uncertainty reflected the temporal context of our classifications. Varying states of recovery from past disturbance may have introduced error in both our expert classifications and SOM clustering outcomes. It is likely that some reaches are in transition between sediment regimes as the channel evolves in response to past floods and other natural and human disturbance(s), and therefore may have been mis-classified. By plotting the color-coded expert-assigned reach observations directly on the converged lattice of an SOM (Figs. 8b and 9c), these “outliers” (i.e., mis-classified reach observations) could be readily identified. Notably, they were often positioned at the boundaries, or transitions, between clusters.

A third source of uncertainty in our sediment regime classifications represents an opportunity for future research. Classical studies have identified relatively frequent, moderate recurrence-interval flow events as the dominant discharge important in governing channel-floodplain form and transporting a majority of the sediment from the watershed (Wolman and Miller, 1960). More recent studies suggest that a wider range of recurrence interval floods are important in governing channel form and sediment flux (Lenzi et al., 2006; Downs et al., 2016). Particularly in bedrock-controlled headwaters, extreme events play a more dominant role in shaping the channel and transporting sediment (Wolman and Gerson, 1978; Lenzi et al., 2006). While the metrics in

our sediment regime classification (e.g., W/D ratio, IR, SSP) are derived for bankfull (Q1.5) stage, and the sediment classifications constitute the continuum of regimes characteristic of higher-frequency, low- to moderate-magnitude discharge (Q2 to Q50), we recognize that extreme events ($>Q50$) can exert significant controls on channel and floodplain response – both in terms of the event itself, and by influencing channel change through post-flood recovery phases (Wolman and Gerson, 1978). Extreme events have legacy impacts on channel adjustment that can persist long after the event by altering boundary conditions including valley slopes, source sediment volumes, landscape and streambank vegetation conditions, and instream large woody debris densities (Dethier et al., 2016). The current sediment regime may be a manifestation of recovery from a past extreme event, more so than characteristic of the bankfull-flow regime (Dethier et al., 2016). To some degree, the different outcomes of our coarse-tune versus fine-tune SOMs may have been reflecting these contrasting temporal and spatial contexts for reach-scale sediment production, transport and deposition, but more study would be needed.

5.3. SOM advantages for visualization

The SOM and its component planes have advantages over traditional statistical methods when visualizing the multivariate features that interact in nonlinear ways to manifest in a given sediment regime. The reduction of multi-dimensional data to a two-dimensional lattice (e.g., Figs. 8b and 9c) simplified the data analysis, and component planes (Figs. 6b and S2) and bar plots (Figs. 7b–d and 9b) provided insight into which variable (or combinations of variables) may be a governing factor(s) in any particular cluster (i.e., sediment regime).

By applying a space-for-time substitution, the converged lattice also represents a kind of process domain space (Montgomery, 1999) that can help visualize the transition of a channel reach from one sediment regime to another as it progresses through channel evolution stages (Fig. 10). For example, consider a low-gradient, gravel-dominated, riffle-pool reach with good connection to its floodplain (i.e., $IR < 1.3$) – all conditions that suggest a quasi-equilibrium state (channel evolution

stage I) characterized by a CEFD sediment regime. If this reach was subjected to channelization and dredging that lead to channel incision ($IR > 1.3$) and floodplain disconnection, it would move to stage II, characterized by UST and FSTCD regimes (Fig. 10a and c). The individual component planes for IR and W/D ratio demonstrate monotonic trends in the lattice-vertical and lattice-horizontal dimensions that are consistent with this idea. The pre-disturbance reach would plot near the top-center of the lattice. Upon dredging, this same reach would shift vertically downward and right on the lattice to areas characterized by higher IR values. With subsequent widening, this reach would move lattice-left to a region typified by higher W/D ratios (and greater numbers of depositional bars; Fig. S2). As channel widening reduces stream competence leading to progressive aggradation, this reach might transition to a more transport-limited state – moving further lattice-left and -up toward a region characterized by increasing numbers of depositional bars and lower W/D ratio. Finally, with progressive channel-narrowing, the channel may return to a quasi-equilibrium state (stage V) and return once again to the top-center of the lattice. Thus, the SOM lattice provides a way to explicitly consider and “map” the trajectory of shifting geomorphic process domains with time.

5.4. Management implications

Classifying the current sediment regime of river reaches is of value for water resource managers to highlight the potential for impacts to property, water quality and habitat, and to inform prioritization schemes for allocation of limited resources (Brierley and Fryirs, 2005; Kline and Cahoon, 2010; Thorp et al., 2013). Vertically-disconnected reaches have greater propensity for vertical and lateral channel adjustments with the potential to impact adjacent built infrastructure. In confined settings of the glacially-conditioned Northeastern US, roads, rail berms, bridges and culverts are commonly located within narrow, steep river valleys. In Vermont, this transportation infrastructure is commonly located adjacent to vertically-disconnected CST reaches and is at enhanced risk of damage during moderate to extreme events (Anderson et al., 2017). In unconfined reaches, varying degrees of

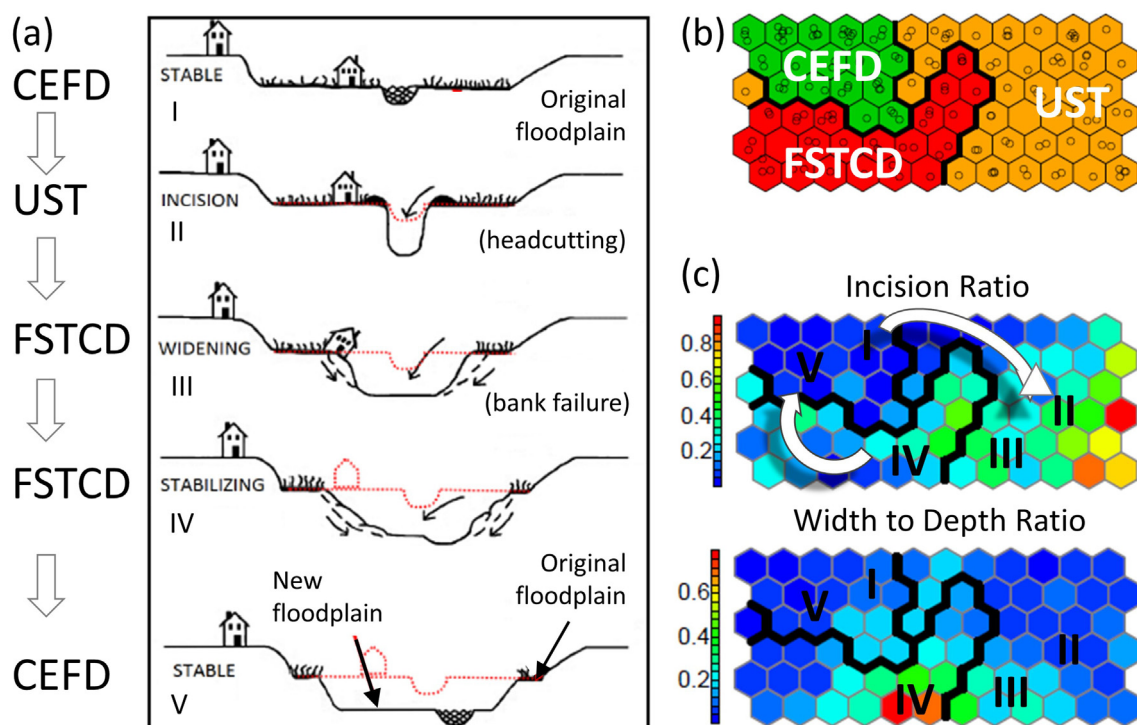


Fig. 10. Representation of (a) sediment regime classes by channel evolution stage (Schumm et al., 1984) superimposed on (b) the fine-tune SOM lattice; and (c) SOM component planes.

vertical disconnection from the floodplain would subject a channel to increased magnitudes of SSP, particularly during low-frequency flood events, with implications for enhanced erosion. Fig. 11 is based on a case of contiguous reaches in the Mad River watershed in central Vermont, where reach A (UST) has been subjected to historic dredging, channel straightening and berming to the extent that it has become disconnected from the floodplain ($IR = 2.6$). While a nearby downstream reach of similar drainage area (reach B; CEFD) and valley slope and confinement remained relatively unmodified and well connected to the floodplain ($IR = 1.0$). A range of storm flows was simulated using a 1D hydraulic model for a regional flood study (Dubois and King, Inc., 2017), and main channel SSP was computed as the product of average shear stress and average velocity. At the 2.3-year RI peak discharge, the relative difference in channel SSP between reaches A and B is largely the result of differing channel configurations. In the entrenched cross section (reach A), a steeper slope (from historic channel straightening practices) and slightly greater hydraulic radius (more efficient cross section) minimizes friction (due to smaller wetted perimeter) leading to higher velocities and greater SSP. For the range of flows above a 2.3-year RI, however, the channel relationship to floodplain becomes most important. Since modeled flood flows of all stages above Q2.3 were able to access the floodplain in the non-entrenched reach B, the channel-bed SSP has much lower magnitude across the array of peak flows than the entrenched cross section of reach A. Conversely, given the degree of incision and entrenchment at reach A, SSP continues to rise steadily until overtopping of the bank occurs somewhere between a Q100 and Q500 flood peak. Magnitudes of SSP at the reach A cross section greatly exceed the 300 W m^{-2} value suggested by Magilligan (1992) as a threshold for major channel adjustment. Fig. 11 illustrates the enhanced potential of incised and entrenched (i.e., UST) channels to serve as a source of sediment to downstream reaches.

CEFD reaches that are well-connected with the floodplain can be prioritized for corridor protection strategies in municipal or regional planning and zoning to maintain their floodplain storage function. On the other hand, FSTCD reaches that are presently disconnected from the floodplain may be prioritized for conservation easements to curtail river management and allow the unfolding channel evolution process to create new floodplain as an “attenuation asset” (Kline, 2010). Particularly, where such reaches are located upstream of developed areas with a greater degree of channel encroachment, they may be targeted for protection and worthy of public investment for the attenuation of flood peaks and associated reduction in flooding hazards to downstream communities (Kline and Cahoon, 2010; Watson et al., 2016).

In the northeastern US, where magnitude, frequency and intensity of extreme storm events are projected to increase (Guilbert et al., 2014), vertically-disconnected channels will have an enhanced potential to serve as a source of sediment to downstream reaches. CST reaches are vulnerable to increased fine sediment export under extreme events

where these channels impinge upon hillslopes and high terraces comprised of glaciolacustrine or glacial till deposits (Yellen et al., 2014; Dethier et al., 2016). Since, the trajectory of SSP rise with storm recurrence interval is much steeper for incised and entrenched UST and FSTCD reaches, it can be inferred that they will have greater potential to export sediment than CEFD reaches. Coarse sediment will have the potential to aggrade and drive lateral adjustments and avulsions in downstream reaches, while fine sediments will be carried to receiving waters and further degrade water quality.

To address water quality concerns on a river network scale, this sediment regime classification approach could be used to identify reaches that are disproportionately responsible for loading of coarse and fine sediments. For example, streambank erosion has been identified as a source of phosphorus contributing to harmful algal blooms in Lake Champlain in the northwestern region of Vermont (Isles et al., 2015). In the Total Maximum Daily Load plan, estimates of phosphorus loading from streambanks are based on the dominant reach-based channel evolution stage at a HUC 12 scale (USEPA, 2016). Our algorithm could be used to refine estimates of streambank sediment loading at a more granular scale to identify “hot spots” (McClain et al., 2003) and to optimize best management practices for the reduction of sediment and nutrient loading.

6. Conclusions

Multivariate stream geomorphic assessment data have been clustered into sediment process domains that constitute net sources or sinks of coarse and fine sediment on a mean annual temporal scale (i.e., Q1.5 discharge) using a two-stage Self-Organizing Map (SOM). The iterative process of streamlining input parameters and training the SOM identified a parsimonious set of geomorphic and hydraulic variables that meaningfully separated reaches into these sediment regimes. Our results illustrate the importance of landscape controls including bedrock knickpoints and glaciogenic landforms in governing downstream trends in sediment regime, as well as the impacts of channel-floodplain encroachments and modifications that have been superimposed on these inherited glacial landform effects.

While this classification scheme has been applied to characterize sediment process domains in the glacially-conditioned and mountainous areas of northeastern US, the framework is transferable to other regions (utilizing additional or alternate independent variables). The geomorphic and hydraulic variables used to cluster the studied reaches were similar to parameters commonly inventoried during assessment protocols in widespread. As channels evolve over time in response to stressors or management practices, these data-driven, nonparametric clustering tools can be quite easily updated with new assessment results, supporting an adaptive approach to river corridor management that offers data visualization capabilities.

To our knowledge, this current study is the first application of a neural network to examine geomorphic data for a range of stream types and to classify a reach-based sediment regime that explains the nature of the adjustment (vertical, lateral) within the trajectory of channel evolution. Our results extend the supply-limited to transport-limited continuum of reach types suggested by Montgomery and Buffington (1997), through the additional dimension of a channel's increasing degree of vertical disconnection from the floodplain that can result from a variety of natural and human disturbances. Through its effect on channel stream power, this vertical-lateral connectivity condition can influence the sediment transport regime in channels and has implications for inundation and erosion flooding hazards, as well as water quality and ecological integrity in the active river corridor.

Future work will explore automation of this algorithm, and variable weighting of input parameters informed by a panel of domain experts. Linking this algorithm to existing stream geomorphic assessment data in a GIS will enable model predictions statewide and the analysis of potential autocorrelation of sediment regimes with distance along stream

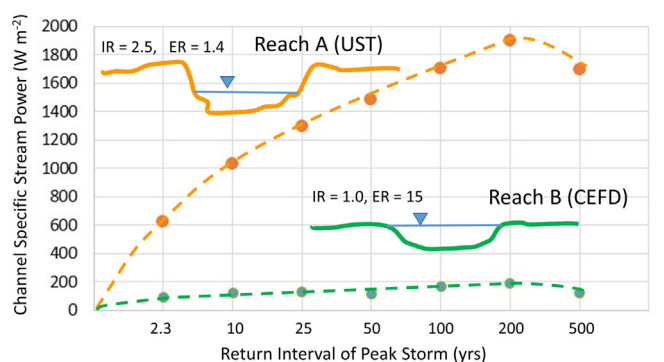


Fig. 11. Channel-bed SSP estimated for a range of modeled return interval storms in contiguous reaches of the Mad River, VT with differing channel configurations (IR, ER).

networks. The anticipated framework will facilitate scenario testing to evaluate how sediment transport regimes of a given reach (or river network) might shift in the event of future channel and floodplain manipulation or restoration, or in response to regional changes in climate. The GIS framework could also be used to forecast estimates of channel adjustment to optimize best management practices for the reduction of sediment and nutrient loading from streambanks.

Declaration of competing interest

The authors declare the following financial interests/personal relationships which may be considered as potential competing interests: KLU has an interest in South Mountain Research & Consulting, a geologic consulting firm, which conducted the stream geomorphic assessments. MK has an interest in Fluvial Matters, LLC.

Acknowledgements

The authors are grateful to Dr. Francesco Brardinoni and a second reviewer (anonymous) for comments and suggestions that have greatly improved the manuscript. This material is based upon work supported by the National Science Foundation under Vermont EPSCoR Grant Nos. EPS-1101317 and NSF OIA 1556770. The first author was partially supported using Federal funds under NA180AR4170099 from the National Oceanic and Atmospheric Administration National Sea Grant College Program, U.S. Department of Commerce. The statements, findings, conclusions, and recommendations are those of the authors and do not necessarily reflect the views of National Science Foundation, Vermont EPSCoR, Sea Grant, NOAA, or the U.S. Department of Commerce. Original geomorphic assessments completed by the first author were supported in part by grants from the FEMA Hazard Mitigation program, the Lake Champlain Basin Program, and the Vermont Agency of Natural Resources. The authors are grateful to Dr. John Field of Field Geology Services for assessment data from two reaches, and to Dubois and King, Inc. for HEC-RAS modeling results underlying Fig. 11. Original stream geomorphic assessment data can be found at <https://anrweb.vt.gov/DEC/SGA/Default.aspx>.

Appendix A. Supplementary data

Supplementary data to this article can be found online at <https://doi.org/10.1016/j.geomorph.2021.107684>.

References

- Alvarez-Guerra, M., González-Piñuela, C., Andrés, A., Galán, B., Viguri, J.R., 2008. Assessment of Self-Organizing Map artificial neural networks for the classification of sediment quality. *Environ. Int.* 34 (6), 782–790. <https://doi.org/10.1016/j.envint.2008.01.006>.
- Anderson, M.J., 2001. A new method for non-parametric multivariate analysis of variance. *Austral Ecology* 26, 32–46. <https://doi.org/10.1111/j.1442-9993.2001.01070.pp.x>.
- Anderson, I., Rizzo, D.M., Huston, D.R., Dewoolkar, M.M., 2017. Stream power application for bridge damage probability mapping based on empirical evidence from Tropical Storm Irene. *Bridg. Eng.* 22 (5), 05017001. [https://doi.org/10.1061/\(ASCE\)BE.1943-5592.0001022](https://doi.org/10.1061/(ASCE)BE.1943-5592.0001022).
- Andrews, E.D., 1983. Entrainment of gravel from naturally sorted riverbed material. *Geol. Soc. Amer. Bull.* 94, 1225–1231.
- Ballantyne, C.K., 2002. Paraglacial geomorphology. *Quat. Sci. Rev.* 21, 1935–2017.
- Benda, L., Dunne, T., 1997. Stochastic forcing of sediment supply to channel networks from landsliding and debris flow. *Water Resour. Res.* 33, 2849–2863.
- Besaw, L.E., Rizzo, D.M., Kline, M., Underwood, K.L., Doris, J.J., Morrissey, L.A., Pelletier, K., 2009. Stream classification using hierarchical artificial neural networks: a fluvial hazard management tool. *J. Hydrol.* 373, 34–43. <https://doi.org/10.1016/j.jhydrol.2009.04.007>.
- Bierman, P.R., 2010. Clearcutting, reforestation, and the coming of the interstate: Vermont's photographic record of landscape use and response. In: Webb, R.H., Boyer, D.E., Turner, R.M. (Eds.), *Repeat Photography: Methods and Applications in the Geological and Ecological Sciences*. Island Press, Washington, D.C, pp. 105–116.
- Bierman, P., Lini, A., Zehfuss, P., Church, A., Davis, P.T., Southon, J., Baldwin, L., 1997. Post-glacial ponds and alluvial fans: recorders of Holocene landscape history. *GSA Today* 7 (10), 1–8.
- Bizzi, S., Lerner, D.N., 2013. The use of stream power as an indicator of channel sensitivity to erosion and deposition processes. *River Res. Appl.* 31, 16–27. <https://doi.org/10.1002/rra.2717>.
- Booth, D.B., 1990. Stream-channel incision following drainage basin urbanization. *Water Resour. Bull. Am. Water Resour. Assoc.* 26 (3), 407–417. <https://doi.org/10.1111/j.1752-1688.1990.tb01380.x>.
- Brakenridge, G.R., Thomas, P.A., Conkey, L.E., Schiferle, J.C., 1988. Fluvial sedimentation in response to postglacial uplift and environmental change, Missisquoi River, Vermont. *Quat. Res.* 30, 190–203. [https://doi.org/10.1016/0033-5894\(88\)90023-3](https://doi.org/10.1016/0033-5894(88)90023-3).
- Brardinoni, F., Hassan, M.A., 2006. Glacial erosion, evolution of river long-profiles, and the organization of process domains in mountain drainage basins of coastal British Columbia. *J. Geophys. Res.* 111, F01013. <https://doi.org/10.1029/2005JF000358>.
- Brardinoni, F., Hassan, M.A., 2007. Glacially induced organization of channel-reach morphology in mountain streams. *J. Geophys. Res.* 112, F03013. <https://doi.org/10.1029/2006JF000741>.
- Brierley, G.J., Fryirs, K.A., 2005. *Geomorphology and River Management: Applications of the River Style Framework*. Blackwell, Oxford 398 pp.
- Brookes, A., 1987. The distribution and management of channelized streams in Denmark. *Regulated Rivers* 1, 3–16.
- Bull, W.B., 1979. Threshold of critical power in streams. *Bull. Geol. Soc. Am.* 90, 453–464.
- Buraas, E.M., Magilligan, F.J., Renshaw, C.E., Dade, W.B., 2014. Impact of reach geometry on stream channel sensitivity to extreme floods. *Earth Surf. Process. Landf.* 39, 1778–1779. <https://doi.org/10.1002/esp.3562>.
- Cereghino, R., Park, Y.-S., 2009. Review of the Self-Organizing Map (SOM) approach in water resources: commentary. *Environ. Model. Softw.* 24, 945–947.
- Chappell, J., 1983. Thresholds and lags in geomorphologic changes. *Aust. Geogr.* 15, 358–366.
- Church, M., Ryder, J., 1972. *Paraglacial sedimentation: a consideration of fluvial processes conditioned by glaciation*. *Geol. Soc. Am. Bull.* 83, 3059–3072.
- Collins, M.J., 2009. Evidence for changing flood risk in New England since the late 20th century. *J. Am. Water Resour. Assoc.* 45 (2), 279–290. <https://doi.org/10.1111/j.1752-1688.2008.00277.x>.
- DeSimone, D., 2000. Surficial Geologic Map of the Arlington and Vermont Portion of the Shushan Quadrangle. Vermont Geological Survey, Waterbury, VT, Open File Report VG00-2. <https://anrweb.vt.gov/PubDocs/DEC/GEO/OpenFileReps/VG002ArlingtonSurf.pdf>.
- Dethier, E., Magilligan, F.J., Renshaw, C.E., Nislow, K.H., 2016. The role of chronic and episodic disturbances on channel-hillslope coupling: the persistence and legacy of extreme floods. *Earth Surf. Process. Landf.* 41 (10), 1437–1447. <https://doi.org/10.1002/esp.3958>.
- Downs, P.W., Soar, P.J., Taylor, A., 2016. The anatomy of effective discharge: the dynamics of coarse sediment transport revealed using continuous bedload monitoring in a gravel-bed river during a very wet year. *Earth Surf. Process. Landf.* 41, 147–161. <https://doi.org/10.1002/esp.3785>.
- Dubois, King, Inc., 2017. Flood study: Mad River Area. <http://centralvtplanning.org/wp-content/uploads/2019/02/Flood-Study-of-the-Mad-River-Area-Report-DK-5.31.17.pdf>.
- Dunne, T., Black, R.D., 1970. Partial area contributions to storm runoff in a small New England watershed. *Water Resour. Res.* 6 (5), 1296–1311.
- Eshghi, A., Houghton, D., Legrand, P., Skaletsky, M., Woolford, S., 2011. Identifying groups: a comparison of methodologies. *Journal of Data Science* 9, 271–291.
- Ferguson, R.I., 2005. Estimating critical stream power for bedload transport calculations in gravel-bed rivers. *Geomorphology* 70 (1–2), 33–41.
- Flores, A.N., Bledsoe, B.P., Cuhaciyan, C.O., Wohl, E.E., 2006. Channel-reach morphology dependence on energy, scale, and hydroclimatic processes with implications for prediction using geospatial data. *Water Resour. Res.* 42, W06412. <https://doi.org/10.1029/2005WR004226>.
- Foster, D.R., Aber, J.D., 2004. *Forests in Time: The Environmental Consequences of 1,000 Years of Change in New England*. Yale University Press, New Haven, CT, 477 pp.
- Frissell, C.A., Liss, W.J., Warren, C.E., Hurley, M.D., 1986. A hierarchical framework for stream habitat classification: viewing streams in a watershed context. *Environ. Manag.* 10 (2), 199–214. <https://doi.org/10.1007/BF01867358>.
- Fryirs, K., 2013. (Dis)Connectivity in catchment sediment cascades: a fresh look at the sediment delivery problem. *Earth Surf. Process. Landf.* 38, 30–46. <https://doi.org/10.1002/esp.3242>.
- Fryirs, K.A., Brierley, G.J., Preston, N.J., Kasai, M., 2007. Buffers, barriers and blankets: the (dis)connectivity of catchment-scale sediment cascades. *Catena* 70, 49–67. <https://doi.org/10.1016/j.catena.2006.07.007>.
- Fytillis, N., Rizzo, D.M., 2013. Coupling self-organizing maps with a Naive Bayesian classifier: stream classification studies using multiple assessment data. *Water Resour. Res.* 49, 7747–7762. <https://doi.org/10.1002/2012WR013422>.
- Gartner, J.D., Dade, W.B., Renshaw, C.E., Magilligan, F.J., Buraas, E.M., 2015. Gradients in stream power influence lateral and downstream sediment flux in floods. *Geology* 43 (11), 983–986. <https://doi.org/10.1130/G36969.1>.
- Guilbert, J., Beckage, B., Winter, J.M., Horton, R.M., Perkins, T., Bombliès, A., 2014. Impacts of projected climate change over the Lake Champlain Basin in Vermont. *J. Appl. Meteorol. Climatol.* 53, 1861–1875. <https://doi.org/10.1175/JAMC-D-13-0338.1>.
- Guilbert, J., Betts, A.K., Rizzo, D.M., Beckage, B., Bombliès, A., 2015. Characterization of increased persistence and intensity of precipitation in the Northeastern United States. *Geophys. Res. Lett.* 42, 1888–1893. <https://doi.org/10.1002/2015GL063124>.
- Harrelson, C.C., Rawlins, C.L., Potyondy, J., 1994. *Stream channel reference sites: an illustrated guide to field technique*. U.S. Department of Agriculture, Forest Service, Rocky Mountain Forest and Range Experiment Station, Fort Collins, CO, General Technical Report RM-245, 61 pp. https://www.fs.fed.us/rm/pubs_rm/rm_gtr245.pdf.
- Isles, P.D.F., Giles, C.D., Gearhart, T.A., Xu, Y., Druschel, G.K., Schroth, A.W., 2015. Dynamic internal drivers of a historically severe cyanobacteria bloom in Lake Champlain

- revealed through comprehensive monitoring. *J. Great Lakes Res.* 41 (3), 818–829. <https://doi.org/10.1016/j.jglr.2015.06.006>.
- Jaquith, S., Kline, M., 2001. Vermont Regional Hydraulic Geometry Curves. Vermont Water Quality Division, Waterbury, VT http://www.anr.state.vt.us/dec/waterq/rivers/docs/rv_hydraulicgeocurves.pdf.
- Jaquith, S., Kline, M., 2006. Vermont Regional Hydraulic Geometry Curves. Vermont Water Quality Division, Waterbury, VT <http://dec.vermont.gov/sites/dec/files/wsm/rivers/docs/assessment-protocol-appendices/J-Appendix-J-06-Hydraulic-Geometry-Curves.pdf>.
- Kline, M., 2010. Vermont ANR River Corridor Planning Guide: To Identify and Develop River Corridor Protection and Restoration Projects. Vermont Agency of Natural Resources, Waterbury, VT https://dec.vermont.gov/sites/dec/files/wsm/rivers/docs/rv_rivercorridorguide.pdf.
- Kline, M., Cahoon, B., 2010. Protecting river corridors in Vermont. *J. Am. Water Resour. Assoc.* 46, 227–236. <https://doi.org/10.1111/j.1752-1688.2010.00417.x>.
- Kline, M., Alexander, C., Pytlík, S., Jaquith, S., Pomeroy, S., 2009. Vermont Stream Geomorphic Assessment Protocol Handbooks. Vermont Agency of Natural Resources, Waterbury, VT <http://dec.vermont.gov/watershed/rivers/river-corridor-and-floodplain-protection/geomorphic-assessment>.
- Knighton, D., 1998. *Fluvial Forms and Processes*. Routledge, New York, NY, 383 pp.
- Kohonen, T., 2001. *Self-Organizing Maps*. Springer, Berlin–Heidelberg, Germany, p. 502.
- Kohonen, T., 2013. Essentials of the self-organizing map. *Neural Netw.* 37, 52–65. <https://doi.org/10.1016/j.neunet.2012.09.018>.
- Lea, D.M., Legleiter, C.J., 2016. Mapping spatial patterns of stream power and channel change along a gravel-bed river in northern Yellowstone. *Geomorphology* 252, 66–79. <https://doi.org/10.1016/j.geomorph.2015.05.033>.
- Lenzi, M.A., Mao, L., Comiti, F., 2006. Effective discharge for sediment transport in a mountain river: computational approaches and geomorphic effectiveness. *J. Hydrol.* 326, 257–276. <https://doi.org/10.1016/j.jhydrol.2005.10.031>.
- Leopold, L.B., 1994. *A View of the River*. Harvard University Press, Cambridge, Massachusetts, p. 320.
- Lisenby, P.E., Fryirs, K., 2016. Catchment- and reach-scale controls on the distribution and expectation of geomorphic channel adjustment. *Water Resour. Res.* 52, 3408–3427. <https://doi.org/10.1002/2015WR017747>.
- Livers, B., Wohl, E., 2015. An evaluation of stream characteristics in glacial versus fluvial process domains in the Colorado Front Range. *Geomorphology* 231, 72–82.
- Magilligan, F.J., 1992. Thresholds and the spatial variability of flood power during extreme floods. *Geomorphology* 5, 373–390.
- Magilligan, F., Haynie, H., Nislow, K., 2008. Channel adjustments to dams in the Connecticut River basin: implications for forested mesic watersheds. *Ann. Assoc. Am. Geogr.* 98, 267–284.
- Mangiameli, P., Chen, S.K., West, D., 1996. A comparison of SOM neural network and hierarchical clustering methods. *Eur. J. Oper. Res.* 93 (2), 402–417.
- McClain, M.E., Boyer, E.W., Dent, C.L., Gergel, S.E., Grimm, N.B., Groffman, P.M., Hart, S.C., Harvey, J.W., Johnston, C.A., Mayorga, E., McDowell, W.H., Pinay, G., 2003. Biogeochemical hot spots and hot moments at the interface of terrestrial and aquatic ecosystems. *Ecosystems* 6, 301–312. <https://doi.org/10.1007/s10021-003-0161-9>.
- Montgomery, D.R., 1999. Process domains and the river continuum. *J. Am. Water Resour. Assoc.* 35 (2), 397–410. <https://doi.org/10.1111/j.1752-1688.1999.tb03598.x>.
- Montgomery, D.R., Buffington, J.M., 1997. Channel-reach morphology in mountain drainage basins. *Geol. Soc. Am. Bull.* 109 (5), 596–611. [https://doi.org/10.1130/0016-7606\(1997\)109<0596:CRMIMD>2.3.CO;2](https://doi.org/10.1130/0016-7606(1997)109<0596:CRMIMD>2.3.CO;2).
- Nanson, G.C., Croke, J.C., 1992. A genetic classification of floodplains. *Geomorphology* 4 (6), 459–486. [https://doi.org/10.1016/0169-555X\(92\)90039-Q](https://doi.org/10.1016/0169-555X(92)90039-Q).
- Noe, G.B., Hupp, C.R., 2005. Carbon, nitrogen, and phosphorus accumulation in floodplains of Atlantic coastal plain rivers, USA. *Ecol. Appl.* 15 (4), 1178–1190. <https://doi.org/10.1890/04-1677>.
- Oksanen, J., Blanchet, F.G., Friendly, M., Kindt, R., Legendre, P., McGlinn, D., Minchin, P.R., O'Hara, R.B., Simpson, G.L., Solymos, P., Henry, M., Stevens, H., Szöcs, E., Wagner, H., 2017. *vegan: community ecology package*. R package version 2.4-3. <https://CRAN.R-project.org/package=vegan>.
- Park, Y.-S., Cereghino, R., Compin, A., Lek, S., 2003. Applications of artificial neural networks for patterning and predicting aquatic insect species richness in running waters. *Ecol. Model.* 160, 265–280. <https://doi.org/10.1016/j.ecoimf.2015.08.011>.
- Parker, C., Clifford, N.J., Thorne, C.R., 2011. Understanding the influence of slope on the threshold of coarse grain motion: revisiting critical stream power. *Geomorphology* 126, 51–65. <https://doi.org/10.1016/j.geomorph.2010.10.027>.
- Parker, C., Thorne, C.R., Clifford, N.J., 2014. Development of ST:REAM: a reach-based stream power balance approach for predicting alluvial river channel adjustment. *Earth Surf. Process. Landf.* 40, 403–413. <https://doi.org/10.1002/esp.3641>.
- Pearce, A.R., Rizzo, D.M., Mouser, P.J., 2011. Subsurface characterization of groundwater contaminated by landfill leachate using microbial community profile data and a non-parametric decision making process. *Water Resour. Res.* 47 (6), W06511. <https://doi.org/10.1029/2010WR009992>.
- Pearce, A.R., Rizzo, D.M., Watzin, M.C., Renschel, G.K., 2013. Unraveling associations between cyanobacteria blooms and in-lake environmental conditions in Missisquoi Bay, Lake Champlain, USA, using a modified self-organizing map. *Environ. Sci. Technol.* 47, 14267–14274. <https://doi.org/10.1021/es403490g>.
- Pfankuch, D.J., 1975. *Stream Reach Inventory and Channel Stability Evaluation*. U.S. Department of Agriculture Forest Service, Region 1, Missoula, Montana.
- Phillips, J.D., 2003. Sources of nonlinearity and complexity in geomorphic systems. *Prog. Phys. Geogr.* 26, 339–361. <https://doi.org/10.1191/030913303pp340ra>.
- Phillips, R.T.J., Desloges, J.R., 2014a. Glacially conditioned specific stream powers in low-relief river catchments of the southern Laurentian Great Lakes. *Geomorphology* 206, 271–287. <https://doi.org/10.1016/j.geomorph.2013.09.030>.
- Phillips, R.T.J., Desloges, J.R., 2014b. Alluvial floodplain classification by multivariate clustering and discriminant analysis for low-relief glacially conditioned river catchments. *Earth Surf. Process. Landf.* 40, 756–770. <https://doi.org/10.1002/esp.3681>.
- Pickup, G., Rieger, W.A., 1979. A conceptual model of the relationship between channel characteristics and discharge. *Earth Surf. Process. Landf.* 4, 37–42. <https://doi.org/10.1002/esp.3290040104>.
- Poff, N.L., Allan, J.D., Bain, M.B., Karr, J.R., Prestegard, K.L., Richter, B.D., Sparks, R.E., Stromberg, J.C., 1997. The natural flow regime: a paradigm for river conservation and restoration. *BioScience* 47, 769–784. <https://doi.org/10.2307/1313099>.
- R Core Team, 2017. *R: A Language and Environment for Statistical Computing*. R Foundation for Statistical Computing, Vienna, Austria <http://www.R-project.org/>.
- Randall, A.D., 1996. Mean annual runoff, precipitation, and evapotranspiration in the glaciated northeastern United States, 1951–1980. U.S. Geological Survey, Open-File Report 96-395.
- Ratcliffe, N.M., Stanley, R.S., Gale, M.H., Thompson, P.J., Walsh, G.J., 2011. Bedrock geologic map of Vermont. U.S. Geological Survey Scientific Investigations Map 3184 <http://www.anr.state.vt.us/dec/geo/StateBedrockMap2012.htm>.
- Raven, P.J., Holmes, N., Dawson, F.H., Fox, P.J.A., Everard, M., Fozzard, I.R., Rouen, K.J., 1998. River habitat quality: the physical character of rivers and streams in the UK and Isle of Man. Environment Agency, River Habitat Survey Report No. 2. <http://www.environmentdata.org/archive/ealit:1913>.
- Rice, S.P., Church, M., 1998. Grain size along two gravel-bed rivers: Statistical variation, spatial pattern and sedimentary links. *Earth Surf. Process. Landf.* 23, 345–363. [https://doi.org/10.1002/\(SICI\)1096-9837\(199804\)23:4<345::AID-ESP850>3.0.CO;2-B](https://doi.org/10.1002/(SICI)1096-9837(199804)23:4<345::AID-ESP850>3.0.CO;2-B).
- Righini, M., Surian, N., Wohl, E., Marchi, L., Comiti, F., Amponsah, W., Borga, M., 2017. Geomorphic response to an extreme flood in two Mediterranean rivers (northeastern Sardinia, Italy): analysis of controlling factors. *Geomorphology* 290, 184–199. <https://doi.org/10.1016/j.geomorph.2017.04.014>.
- Rinaldi, M., Surian, N., Comiti, F., Bussetini, M., 2013. A method for the assessment and analysis of the hydromorphological condition of Italian streams: the Morphological Quality Index (MQI). *Geomorphology* 180–181, 96–108. <https://doi.org/10.1016/j.geomorph.2012.09.009>.
- Rosgen, D., 1996. *Applied Fluvial Morphology*. Wildland Hydrology Books, Pagosa Springs, CO, 390 pp.
- Schumm, S.A., 2005. *River Variability and Complexity*. Cambridge University Press, New York, NY.
- Schumm, S.A., Rea, D.K., 1995. Sediment yield from disturbed earth systems. *Geology* 23, 391–394.
- Schumm, S.A., Harvey, M.D., Watson, C.C., 1984. *Incised Channels Morphology, Dynamics and Control*. Water Resources Publications, Littleton, CO.
- Shanley, J.B., Denner, J.C., 1999. The hydrology of the Lake Champlain Basin. In: Manley, T. O., Manley, P.L. (Eds.), *Lake Champlain in Transition-From Research Toward Restoration*. American Geophysical Union, Washington, D.C., pp. 41–66. <https://doi.org/10.1029/WS001p0041>.
- Somerville, D.E., Pruitt, B.A., 2004. *Physical stream assessment: a review of selected protocols for use in the Clean Water Act Section 404 program*. U.S. Environmental Protection Agency, Office of Wetlands, Oceans, and Watersheds, Wetlands Division (Order No. 3W-0503-NATX) (Washington, D.C., 213 pp.).
- Stewart, D.P., MacClintock, P., 1969. The surficial geology and Pleistocene history of Vermont. Vermont Geological Survey, Montpelier, VT, Bulletin No. 31.
- Stojkovic, M., Simic, V., Milosevic, D., Mancev, D., Penczak, T., 2013. Visualization of fish community distribution patterns using the self-organizing map: a case study of the Great Morava River system (Serbia). *Ecol. Model.* 248, 20–29. <https://doi.org/10.1016/j.ecolmodel.2012.09.014>.
- Surian, N., Righini, M., Lucia, A., Nardi, L., Amponsah, W., Benvenuti, M., Borga, M., Cavalli, M., Comiti, F., Marchi, L., Rinaldi, M., Viero, A., 2016. Channel response to extreme floods: Insights on controlling factors from six mountain rivers in northern Apennines, Italy. *Geomorphology* 272, 78–91. <https://doi.org/10.1016/j.geomorph.2016.02.002>.
- Thompson, C.J., Croke, J.C., 2013. Geomorphic effects, flood power, and channel competence of a catastrophic flood in confined and unconfined reaches of the Upper Lockyer Valley, Southeast Queensland, Australia. *Geomorphology* 197, 156–169. <https://doi.org/10.1016/j.geomorph.2013.05.006>.
- Thompson, E.H., Sorenson, E.R., 2000. *Wetland, Woodland, Wildland: A Guide to the Natural Communities of Vermont*. University Press of New England, Hanover, NH.
- Thorp, J.H., Flotemersch, J.E., Williams, B.S., Gabanski, L.A., 2013. Critical role for hierarchical geospatial analyses in the design of fluvial research, assessment, and management. *Environ. Monit. Assess.* 185 (9), 7165–7180. <https://doi.org/10.1007/s10661-013-3091-9>.
- Toone, J., Rice, S., Piégay, H., 2014. Spatial discontinuity and temporal evolution of channel morphology along a mixed bedrock-alluvial river, upper Drôme River, southeast France: contingent responses to external and internal controls. *Geomorphology* 205, 5–16. <https://doi.org/10.1016/j.geomorph.2012.05.033>.
- U.S. Environmental Protection Agency, 2016. Phosphorus TMDLs for Vermont segments of Lake Champlain. <https://www.epa.gov/tmdl/lake-champlain-phosphorus-tmdlcommitment-clean-water>.
- datasetUS, Geological Survey, 2018. National water information system. <http://waterdata.usgs.gov/vt/nwis/rt>.
- Vesanto, J., Alhoniemi, E., 2000. Clustering of the self-organizing map. *IEEE Trans. Neural Netw.* 11 (3), 586–600.
- Vesanto, J., Himberg, J., Alhoniemi, E., Parhankangas, J., 2000. SOM Toolbox for Matlab 5. Neural Networks Research Centre, Helsinki University of Technology, Helsinki, Finland, Technical Report A57.
- datasetVT Agency of Natural Resources, 2017. Stream Geomorphic Assessment Data Management System. <https://anrweb.vt.gov/DEC/SGA/Default.aspx>.

- Walling, D.E., 1983. The sediment delivery problem. *J. Hydrol.* 65, 209–237. [https://doi.org/10.1016/0022-1694\(83\)90217-2](https://doi.org/10.1016/0022-1694(83)90217-2).
- Walter, R.C., Merritts, D.J., 2008. Natural streams and the legacy of water-powered mills. *Science* 319 (5861), 299–304. <https://doi.org/10.1126/science.1151716>.
- Watson, K.B., Ricketts, T., Galford, G., Polasky, S., O'Neil-Dunne, J., 2016. Quantifying flood mitigation services: the economic value of Otter Creek wetlands and floodplains to Middlebury, VT. *Ecol. Econ.* 130, 16–24. <https://doi.org/10.1016/j.ecolecon.2016.05.015>.
- Weber, M.D., Pasternack, G.B., 2017. Valley-scale morphology drives differences in fluvial sediment budgets and incision rates during contrasting flow regimes. *Geomorphology* 288, 39–51. <https://doi.org/10.1016/j.geomorph.2017.03.018>.
- Weekes, A.A., Torgersen, C.E., Montgomery, D.R., Woodward, A., Bolton, S.M., 2012. A process-based hierarchical framework for monitoring glaciated alpine headwaters. *Environ. Manag.* 50, 982–997. <https://doi.org/10.1007/s00267-012-9957-8>.
- Wehrens, R., Buydens, L.M.C., 2007. Self- and super-organising maps in R: the kohonen package. *J. Stat. Softw.* 21 (5), 1–19. <https://www.jstatsoft.org/index>.
- Wohl, E., 2010. Mountain Rivers Revisited. American Geophysical Union, Washington, D. C. Water Resources Monograph Series 19, 573 pp., doi:<https://doi.org/10.1029/WM019>.
- Wohl, E., 2018. Geomorphic context in rivers. *Progress in Physical Geography: Earth and Environment* 42 (6), 841–857. <https://doi.org/10.1177/0309133318776488>.
- Wohl, E.E., Bledsoe, B.P., Jacobson, R.B., Poff, N.L., Rathburn, S.L., Walters, D.M., Wilcox, A.C., 2015. The natural sediment regime in rivers: broadening the foundation for ecosystem management. *BioScience* 65, 358–371. <https://doi.org/10.1093/biosci/biv002>.
- Wolman, M.G., 1954. A method of sampling coarse river-bed material. *Transactions of American Geophysical Union* 35, 951–956.
- Wolman, M.G., Gerson, R., 1978. Relative scales of time and effectiveness of climate and watershed geomorphology. *Earth Surf. Process.* 3, 189–208. <https://doi.org/10.1002/esp.3290030207>.
- Wolman, M.G., Miller, J.P., 1960. Magnitude and frequency of forces in geomorphic processes. *J. Geol.* 68, 54–74.
- Yellen, B., Woodruff, J.D., Kratz, L.N., Mabee, S.B., Morrison, J., Martini, A.M., 2014. Source, conveyance and fate of suspended sediments following Hurricane Irene. New England, USA. *Geomorphology* 226, 124–134. doi:<https://doi.org/10.1016/j.geomorph.2014.07.028>.
- Yochum, S.E., Sholtes, J.S., Scott, J.A., Bledsoe, B.P., 2017. Stream power framework for predicting geomorphic change: the 2013 Colorado Front Range flood. *Geomorphology* 292, 178–192. <https://doi.org/10.1016/j.geomorph.2017.03.004>.